Retrospective short-term forecasting experiment in Italy based on the occurrence of strong (fore) shocks

P. Gasperini[1,2], E. Biondini[1], B. Lolli[2], A. Petruccelli[1,3], G. Vannucci[2]

[1]Dipartimento di Fisica e Astronomia, Università di Bologna, Italy

[2]Istituto Nazionale di Geofisica e Vulcanologia, Sezione di Bologna, Italy

[3] Swiss Seismological Service, ETH Zurich, Switzerland

paolo.gasperini@unibo.it, emanuele.biondini2@unibo.it, barbara.lolli@ingv.it,

antonio.petruccelli@sed.ethz.ch, gianfranco.vannucci@ingv.it

Summary

In a recent work we computed the relative frequencies with which strong shocks ($4.0 \leq Mw < 5.0$), widely felt by the population were followed in the same area by potentially destructive main shocks ($Mw \geq 5.0$) in Italy. Assuming the stationarity of the seismic release properties, such frequencies can be tentatively used to estimate the probabilities of potentially destructive shocks after the occurrence of future strong shocks. This allows us to set up an alarm-based forecasting hypothesis related to strong foreshocks occurrence. Such hypothesis is tested retrospectively on the data of a homogenized seismic catalogue of the Italian area against a purely random hypothesis that simply forecasts the target main shocks proportionally to the space-time fraction occupied by the alarms. We compute the latter fraction in two ways a) as the ratio between the average time covered by the alarms in each area and the total duration of the forecasting experiment (60 years) and b) as the same ratio but weighted by the past frequency of occurrence of earthquakes in each area. In both cases the overall retrospective performance of our forecasting algorithm is definitely better than the random case. Considering an alarm duration of three months, the algorithm retrospectively forecasts more than 70% of all shocks with $Mw \geq 5.5$ occurred in Italy from 1960 to 2019 with a total space-time fraction covered by the alarms of the order of 2%. Considering the same space-time coverage, the algorithm is also able to retrospectively forecasts more than 40% of the first main shocks with $Mw \geq 5.5$ of the seismic sequences occurred in the same time interval. Given the good reliability of our results, the forecasting algorithm is set and ready to be tested also prospectively, in parallel to other ongoing procedures operating on the Italian territory.

Abbreviated title: Retrospective forecasting based on foreshocks

Introduction

Even if the deterministic prediction of earthquakes is presently not feasible and perhaps it will never be (Geller et al., 1997), several methods of probabilistic operational forecasting have been proposed in the last decades (see Jordan & Jones, 2010 and Jordan et al., 2011 for an overview). Many of such methods take advantage of the well-known property of earthquakes to cluster in space and time (Mulargia & Geller 2003; Kagan, 2014) and in particular of the possibility that relatively small shocks, occurring in advance (foreshocks) of destructive main shocks, might be used as precursory signal.

Jones & Molnar (1976, 1979) first observed that the property of worldwide strong earthquakes of being preceded by a few days or weeks of smaller shocks could have been used to predict somehow their occurrence. Jones (1984, 1985) noted that in California the occurrence of a weak shock increased of several order of magnitude the probability of occurrence of a main shock in the following hours or days and Agnew & Jones (1991) and Jones (1994) computed the probability of a major earthquake along the San Andreas fault in California, given the occurrence of a potential foreshock nearby the fault. The occurrence of foreshocks was then adopted as one of possible precursor of large earthquakes by the Southern San Andreas Working Group (1991) and Reasenberg (1999a, 1999b) estimated the prospective frequency of potential foreshock being followed by stronger earthquakes in California and worldwide.

In Italy, Caputo et al. (1977, 1983) analysed earthquakes' swarms as forerunners of strong earthquakes, Grandori et al. (1988) proposed an alarm system based on the occurrence of a pair of foreshocks, Console et al. (1993) and Console & Murru (1996) studied the foreshock statistics and their possible relationship to earthquake prediction and Di Luccio et al. (1997) and Console et al. (1999) set up a forecasting hypothesis for the occurrence of earthquakes conditioned by prior events. More recently, Gasperini et al. (2016), by the retrospective analysis of a homogeneous seismic catalogue of the Italian region, computed the relative frequencies with which strong shocks (defined

as 4.0≤Mw<5.0) were followed in the same area by potentially destructive main shocks (defined as Mw≥5.0, 5.5, 6.0). In particular, they found that just after strong shocks, the relative frequency of potentially destructive main shocks in the same area increases with respect to quiet periods by a factor up to about 100000. Then, as time goes by without any main shock occurring, such factor decreases logarithmically down to less than 10 for time windows of months to years. Within one day after the occurrence of a strong shock, the frequencies of main shocks with Mw ≥ 5.0 and Mw ≥ 5.5 range from 5 per cent to 2 per cent while within one month they range from 14 per cent to 6 per cent. Frequencies remain quite stable for about one hour after the strong shock and then start to decrease logarithmically at a rate of about 1 per cent for a doubling of the time elapsed from the strong shock. The frequencies of large main shocks (Mw ≥ 6.0) are generally lower than 1 per cent except from about one month after a strong shock with 4.5 ≤ Mw < 5.0 when they become of the order of 4 per cent, but they decrease well below 1 per cent about two or three months after the strong shock if the main shock did not actually occur in the meantime. About 30 per cent of main shocks have been preceded by strong shocks in the day before, about 50 per cent one in the month before and about 60 per cent in the year before.

All such evidences suggest us to formulate an alarm-based forecasting hypothesis related to the simple occurrence of strong shocks in a given area. In this work we first set up such hypothesis and then optimize it by the retrospective analysis of the HOmogenized instRUmental Seismic catalogue (HORUS) of the Italian area from 1960 to 2019 (Lolli et al., 2020) which is an improved and updated version of the seismic catalogue used by Gasperini et al. (2016).

In our knowledge, this is the first alarm-based forecasting experiments applied to the Italian region after the one by Grandori et al. (1988) cited above and after Console et al. (2010) and Murru et al. (2009) who converted to an alarm-based approach previous probabilistic forecasting studies by Console and Murru (2001) and Console et al. (2003, 2006). In fact, the latter studies, as well as others forecasting efforts in Italy (see Schorlemmer et al., 2010 and Marzocchi et al., 2014 for an overview), mostly based on the Epidemic-Type Aftershock Sequence (ETAS) model (Kagan & Knopoff, 1987,

4

Ogata, 1988), were developed to reproduce at best the general behaviour of future seismicity, not to issue a warning of a possibly impending damaging earthquake.

The present forecasting hypothesis will be possibly submitted for prospective testing and validation to the testing facilities of the Collaboratory Study of Earthquake Predictability (CSEP, Jordan, 2006, Zechar et al., 2009).

Setting up the forecasting hypothesis

We issue an alarm of duration Δt within a circular area (CA) of radius R every time a strong shock with $M_{min} \leq M < M_{max}$ occurs inside the CA. As target events to be forecasted we consider all the shock, with magnitude above a threshold $M_m \geq M_{max}$.

We must note that after the actual occurrence of a target shock, the forecast of further target shocks in the same area and in the following weeks or months is somehow favoured by the strong aftershocks of the previous target event. Hence, we also verify the ability of our method to forecast only the first target shock of each sequence. We then consider also a declustered set of target shocks obtained by eliminating those target shocks occurred within a distance $D = 50$ km and a time window of a year after another target shock of the sequence, even if they are larger than the first target shock of the sequence. This kind of declustering is somehow different with respect to that adopted for example in seismic hazard assessment (e.g. Gardner & Knopoff, 1974, Reasenberg, 1985) in which each sequence is usually represented by the largest shock, even if it is not the first one in the sequence. We choose the declustering space and time windows based on our experience on past Italian seismic sequences but we also checked visually that none possible secondary mainshock remains not declustered. Also note that the chosen declustering windows approximately correspond to those determined by the algorithm of Gardner and Knopoff (1974) for M=5.5.

As source areas we consider a regular tessellation of the Italian territory made of partially overlapping CAs with fixed radius R. Starting from an initial CA, centred at latitude 47º and longitude 7º, we

compute the centres of the neighbour CAs by moving with steps $D = R\sqrt{2}$ both in longitude (from 7º to 19º) and in latitude (from 47º to 36º) covering then the whole Italian area with partial overlapping (Fig. 1).

Based on the results of our previous analysis (Gasperini et al., 2016), we choose a radius $R = 30$ km, as a good compromise between the opposing demands of having short spatial resolution and a sufficiently high number of earthquakes within each CA, so obtaining a total of 695 partially overlapping CAs. However, as the completeness of the seismic catalogue is poor in offshore areas, we consider in our analysis only the CAs within which at least one earthquake with Mw≥4.0 occurred inland from 1600 to 1959 (so as to be independent of the seismicity from 1960 to 2019 that will be used for the retrospective testing and optimization of the forecasting method), according to the CPTI15 catalogue (Rovida et al., 2016, 2020).

According to Gasperini et al. (2016), we consider as target shocks the earthquakes with Mw≥5.0, Mw≥5.5 and Mw≥6.0, which, in Italy, usually cause moderate, heavy and very heavy damage to buildings and none, a few and many victims respectively. Larger thresholds cannot be investigated because only three shocks with Mw ≥6.5 (1976 Friuli with Mw=6.5, 1980 Irpinia with Mw=6.8 and 2016 Norcia with Mw=6.6) occurred during the time interval covered by our seismic catalogue.

We count a success if a target shock occurs during one or more alarm time windows Δt and within one or more CA. On the contrary we count a missed forecast if a target shock occurs outside any alarm window of any CA. According to Molchan (1990, 1991) we compute the miss rate as

$$\nu = \frac{N - h}{N} \tag{1}$$

where h is the number of target events successfully forecasted and N is the total number of target events.

We also compute the total time duration d_c of alarms as the union of all alarm windows within each CA. This can also be computed by multiplying the window length Δt by the number n of issued alarms and then subtracting the sum of time intersections between alarm windows $\cap t_s$

$$d_c = \bigcup \Delta t = n\Delta t - \sum \cap t_s \tag{2}$$

The fraction of time occupied by alarms within each CA is then computed as

$$\tau_c = \frac{d_c}{T} \tag{3}$$

where T is the total duration of the forecasting experiment.

Finally, the overall fraction of space-time occupied by alarms is computed as the average of τ_c over all CAs

$$\tau_u = \frac{1}{M} \sum \tau_c \tag{4}$$

where M is the number of CAs. Note that such definition of fraction of space-time occupied by alarms is consistent with strong shocks occurring in the overlapping region of two adjoining CAs because in such case we sum the alarm fraction of time τ_c for both CAs.

Following Shebalin et al. (2011) we also compute the fraction of space-time occupied by alarms by weighting each alarm with the long-term rate of earthquakes within each CA. We compute such rate based on the data of the CPTI15 catalogue (Rovida et al., 2016, 2020) using different completeness thresholds Mc for different time intervals from 1620 to 1959 (Table 1). We count the numbers of earthquakes $N(Mc)$ above each magnitude threshold Mc occurred within each CA and within the corresponding time interval of completeness $\Delta T(Mc)$. Then we compute for each magnitude threshold the expected rate λ (event/year) of earthquakes with Mw$\geq$4.0, assuming the *b-value* of the frequency-magnitude distribution (Gutenberg & Richter, 1944) equal to 1 (Rovida et al., 2020):

$$\lambda = \frac{N(Mc)}{\Delta T(Mc)} 10^{M_c - 4.0} \tag{5}$$

In each CA, we then compute the average λ_{ave} of rates $\lambda > 0$ from different magnitude thresholds. For those CAs for which such average frequency cannot be computed because there are no earthquakes within the completeness time window of any magnitude threshold, we assign the minimum rate computed overall.

Finally, the weighted fraction of space-time occupied by alarms is computed from all CAs as

$$\tau_w = \frac{\sum \lambda_{ave} \tau_c}{\sum \lambda_{ave}} \qquad (6)$$

See the details of such computations for each CA in Table S1 of the supplemental material.

Dataset used for testing and optimization

To test and optimize our algorithm, we apply it retrospectively to the HOmogenized instRUmental Seismic catalogue (HORUS) of Italian instrumental seismicity from 1960 to 2019 (Lolli et al., 2020). For the time interval from 1960 to 1980, HORUS coincides with the dataset prepared by Lolli et al. (2018) and that can be downloaded from the electronic supplement of such paper. For the period from 1981 to 2019, it is obtained by merging various data sources and homogenizing the magnitudes to Mw as described by Gasperini et al. (2012, 2013). The catalogue used here is updated up to the end of 2019 but we have implemented an automatic procedure able to continuously update such catalogue in near real-time (with daily to hourly updates) through the downloading of new data from on-line sources and the application of magnitude conversions (Lolli et al., 2020). We provide the final catalogue on a web site for public dissemination and the possible prospective testing of the present and other forecasting methods.

The magnitude completeness threshold for the period 1960-1980 has been assessed by Lolli et al. (2018) to be about 4.0 whereas, according to Gasperini et al. (2013), it is definitely lower for the successive time periods. Such thresholds might be definitely larger in offshore areas owing to the large distances from the closest seismic stations, which are usually located on land (excepting for a few instruments deployed on the sea bottom). This is the reason why we only consider earthquakes with Mw≥4.0 occurred within the 190 CAs containing one inland earthquake at least. As our interest is to forecast earthquakes that potentially threaten lives and goods, we also limit the analysis to shocks shallower than 50 km. We show in Fig. S1 of supplemental material the spatial distribution of inland

8

earthquakes from the HORUS catalogue (Lolli et al., 2020) with Mw≥4.0 and depth < 50 km used for testing and optimization and in Fig. S2 the time distribution of magnitudes of all inland earthquakes with depth <50 km.

The catalogue provides uncertainties for all magnitude estimates, ranging from less than 0.1 (for Mw estimated by moment tensor inversion) to about 0.5 (for Mw proxies from body wave magnitude mb observed by a few stations). In general, magnitude and location errors have the effect to increase the randomness of the catalogue and then to penalize skilled forecasting methods with respect to unskilled ones.

Owing to the Gutenberg Richter (1944) law, errors tend on average to overestimate all magnitudes because there are more earthquakes below a given threshold which can be overestimated than earthquakes above the same threshold which can be underestimated. The larger the error the larger the overestimation.

On the other hand, magnitude errors are generally larger for small earthquakes because the latter are observed by less stations and because accurate method of magnitude determination, like moment tensor inversion, cannot be applied to them. This means that in general small earthquakes are overestimated more than larger ones and then that foreshocks are overestimated more than target shocks.

One possible consequence in the present case is that errors in magnitude might improperly increase the number of alarms and then the space-time fraction occupied by alarms, particularly in earlier times when the coverage of seismic networks was coarser, so that to slightly underestimate the real skill of the method. Conversely the number of target shocks should not be affected much by magnitude errors because in HORUS catalogue the most (about 80%) of Mw≥5.0 are accurately computed by moment tensor inversions.

Testing and optimizing the forecasting hypothesis

We here follow the approach proposed by Zechar & Jordan (2008, 2010) based on the so called "Molchan error diagram" (Molchan, 1990, 1991, Molchan & Kagan, 1992). The latter consists of a plot (e.g. Fig. 2) of the miss rate ν (eq. 1) as a function of the fractions of space-time occupied by alarms τ (τ_u of eq. 4 or τ_w of eq. 6). For a paradoxical forecasting method not issuing any alarm, the space-time occupied by alarms is 0 and no target events can be forecasted (all target event are missed) then it is represented by the point $(\tau,\nu) = (0,100\%)$ at the upper left corner of the Molchan diagram. On the other hand, for a forecasting method issuing an alarm at any time and in any place, so occupying the entire space-time volume, no target events are missed and then the forecasting method is represented by the point $(\tau,\nu) = (100\%,0)$ at the lower right corner of the diagram. The points on the diagonal line connecting such two points (e.g. the black continuous line in Fig. 2), with equation

$$\nu = 1 - \tau \qquad (7)$$

indicate the expected performance of a purely random forecasting method that simply forecasts target events proportionally to the space-time fraction occupied by the alarms.

On the diagonal line, the ratio between the success rate and the space-time fraction

$$G = \frac{1 - \nu}{\tau} \qquad (8)$$

is 1 for any τ, while for a skilled forecasting method, located below the line, $G > 1$ represents the "probability gain" factor with respect to the random case.

Following Zechar & Jordan (2008), τ (τ_u or τ_w) can be assumed as the probability of forecasting a target events by chance and then can be used to measure the performance of a forecasting method under the reasonable assumption that the probability of having exactly h successful forecasts over N targets is given by the binomial probability function

$$B(h|N\tau) = \binom{N}{h}(\tau)^h(1 - \tau)^{N-h} \qquad (9)$$

Then the cumulative probability of having by chance h or more successful forecasts is

$$\alpha = \sum_{n=h}^{N} B(n|N\tau) = 1 - \sum_{n=0}^{h-1} B(n|N\tau) \qquad (10)$$

Such statistic allows to measure the skill of a forecasting methods, given the miss rate ν and the fraction of space-time occupied by alarms τ. In particular, the lower the statistic the higher the skill. Moreover, by inverting eq. (10), we can compute the expected miss rate ν at a given τ, for a hypothetical forecasting method with given probability α, and then to plot confidence limits on the Molchan diagram (e.g. the blue, violet and green lines in Fig. 2).

This statistic can be used to validate a forecasting method using a prospective dataset (collected after the final fixing of the forecasting hypothesis) but even to optimize the forecasting hypothesis by searching the values of the parameters of the forecasting algorithm (if any) for which the statistic is minimum, by using a retrospective dataset.

A given forecasting method with fixed parameter values is represented by a single point (τ,ν) on the Molchan diagram. However, one can even consider curves (Molchan trajectories) connecting different points referred to the same general forecasting approach but obtained by varying one of the free parameters of the forecasting algorithm. In our case we can vary the alarm time window Δt from 0 to the total duration T of the experiment. In this way, we span the total space-time occupied by the alarms and correspondingly the number of successful forecasts, which increase with increasing Δt.

In the light of such definition, the diagonal line in the Molchan diagram can be seen as the Molchan trajectory of a purely random forecasting method. If a forecasting method performs better than the random one, its trajectory mainly lies in the lower left half of the Molchan diagram below the random line.

Zechar & Jordan (2008, 2010) proposed to use as a measure of the performance of an alarm-based forecasting method the integral of the success rate function $1 - \nu_f(\tau)$ normalized to the alarm space-time coverage τ

$$a_f(\tau) = \frac{1}{\tau} \int_0^\tau [1 - \nu_f(t)] dt \qquad (11)$$

11

As the integral corresponds to the area above the Molchan random trajectory, the statistic was named

Area Skill (AS) score. The AS score is normalized so that its value ranges between 0 and 1: the larger

the statistic the better the performance.

The expected value of the AS score for a purely random method can be derived by substituting the

equation (7) of the random line $\nu_f(t) = 1 - t$ in equation (11). This gives

$$\langle a_f(\tau) \rangle = \frac{1}{\tau} \int_0^\tau [1 - (1 - t)] dt = \frac{1}{\tau} \frac{\tau^2}{2} = \frac{\tau}{2} \tag{12}$$

Such expectance function is represented in a plot as a function of τ by a straight line connecting the

axes origin (0,0) with the point (100%, 50%) (e.g. the black line in Fig. 3). In such plot, the skilled

forecasting methods lie above such random line.

Zechar & Jordan (2008, 2010) explored the AS score distribution and found that, for a continuous

alarm function, the AS score at $\tau = 1$ is asymptotically Gaussian with a mean of 1/2 and a variance

of 1/(12N). They also found that the kurtosis excess is -6/(5N) and hence, for N of the order of a

dozen at least, the Gaussian approximation provides a good estimate of confidence bounds. Finally,

they argued that even if the area skill score can be computed for any τ, the power of the test tends to

increase with increasing τ and therefore it is the best to use $a_f(\tau = 1)$ for hypothesis testing.

Results of retrospective testing

In Fig. 2 we show the Molchan trajectories for all target shocks (35) with Mw≥5.5 (not-declustered)

preceded by strong shocks with 4.4≤Mw<4.8, by varying Δt from a width of a few seconds to the

total duration *T*=60 years of the catalogue. Red and dark blue lines refer to the unweighted (τ_u) and

weighted (τ_w) fractions of space-time occupied by alarms respectively (see in Table S2 in

supplemental material the numerical values of plotted curves).

The adopted foreshock Mw range (Mw=4.6±0.2) was chosen after a comparative analysis of the

relative performance of various ranges with lower and upper magnitude bounds varying from the

completeness threshold of the catalogue (Mw=4.0) to the minimum magnitude of target shocks (Mw=5.0). Such analysis was aimed at maximizing the overall AS score and at the same time minimizing the total number of alarms (Fig. 4).

Both the red and dark blue lines in Fig. 1 lie well below the α =1% confidence curve (green) for all explored Δt. All the target shocks are successfully forecasted (v =0) for Δt=20 years (corresponding to $\tau_u = 32\%$ and $\tau_w = 51\%$) or larger. For Δt=1 year, about 83% of target shocks (29) are successfully forecasted, with space-time coverages $\tau_u = 3.3\%$ and $\tau_w = 6.3\%$. 40% of target shocks (14) are forecasted with Δt=1 day for which $\tau_u = 0.01\%$ and $\tau_w = 0.03\%$. The AS diagram in Fig. 3 (see Table S2 in supplemental material for numerical values) confirms such good performance with the scores of the forecasting method (red and dark blue lines) well above the random expectation (black) and the 1% confidence line (green) for any Δt. The overall AS scores $a_f(\tau = 1) = 0.96\pm0.05$ and $a_f(\tau_w = 1) = 0.94\pm0.05$, based on the Student's t-test, are significantly larger than the expectance of a random method (0.5) with significance level (s.l.) $\ll$0.01.

As noted above the aftershocks produced by the first target shocks of seismic sequence may significantly contribute to forecast subsequent target shocks with Mw≥5.5 within the same sequence. We then proceed to analyse in the same way the declustered set of target shocks with Mw≥5.5 obtained by discarding all target shocks occurred within a spatial distance R=50 km and a time window of a year after the first and all subsequent Mw≥5.5 shocks of the sequence. This reduces the number of considered target shocks with Mw≥5.5 from 35 to 14.

In Fig. 5 and 6 we report the same plots as in Fig. 2 and 3 but for the (declustered) set of only the first target shocks with Mw≥5.5 of each sequence (see Table S3 in supplemental material for numerical values). The performance is worse than for the not-declustered set but remains well below the random line and the α=1% confidence curve in the Molchan diagram of Fig. 5 and also well above the α =1% confidence line of AS diagram of Fig. 6. Even in this case all 14 target shocks are successfully forecasted with Δt=20 years or larger. For Δt=1 year, 64% of target shocks (9) are forecasted and

29% (4) for Δt=1 day. The overall AS score $a_f(\tau_u = 1) = 0.93\pm0.08$ and $a_f(\tau_w = 1) = 0.87\pm0.08$ are lower than for the not-declustered set but anyhow they are significantly larger than the expectance (0.5) of a random method with s.l. $\ll 0.01$.

In Figs. S3, S4, S5 and S6 of supplemental material, we report the same plots of Fig. 2, 3, 5 and 6 for target shocks with Mw$\geq$5.0 (numerical values in Tables S4 and S5). The performance is definitely worse than for Mw$\geq$5.5 but still better than the 1% confidence limit. In particular, even for Δt =60 years, only 89 over 98 (91%) target shocks for the not-declustered set and only 36 over 44 (82%) for the declustered set are successfully forecasted. The reason is that even when Δt is equal to the total duration of the catalogue, in some CAs there remains a fraction of time (before the first strong shock) without any strong shock and then without any alarm. Actually, the maximum fraction of space-time occupied by alarms (τ_u) is only about 44% of the total space-time and 9 target shocks with Mw$\geq$5.0 occurred in the remaining 56%. Here, the last part of the Molchan trajectories, consisting of a linear decrease from the last point defined by the algorithm ($\tau_u = 44\%$ and $\tau_w = 62\%$ with $\nu = 9\%$ for not-declustered and 18% for declustered) to the lower left corner ($\tau = 100\%$, $\nu = 0$), can be interpreted as the application to the remaining earthquakes, not predicted by any foreshock, of a purely random forecasting method with success rate proportional to the fraction of the remaining space-time region not covered by our forecasting algorithm.

The overall AS scores are $a_f(\tau_u = 1) = 0.89\pm0.03$ and $a_f(\tau_w = 1) = 0.85\pm0.03$ for the not-declustered set and $a_f(\tau = 1) = 0.78\pm0.04$ and $a_f(\tau_w = 1) = 0.70\pm0.04$ for the declustered set. In all cases they are significantly larger than the expectance (0.5) of a random method with s.l. $\ll 0.01$.

In Figs. S7, S8, S9 and S10 of the supplemental material, we also report the plots for targets with Mw$\geq$6.0 (see numerical values in Tables S6 and S7). The performance is similar to that for Mw$\geq$5.5 but as the number of target events is smaller (10 not-declustered and 7 declustered), the power of the tests and the reliability of possible inferences are relatively poorer. This is actually reflected by the fact that the confidence limits in this case are relatively close to the Molchan and AS trajectories.

All not-declustered targets are successfully forecasted with $\Delta t = 20$ years, 80% with $\Delta t = 1$ year and 50% with $\Delta t = 1$ day. For declustered targets, the corresponding forecasting rates are 100%, 71% and 43% respectively. The overall AS scores are $a_f(\tau_u = 1) = 0.95 \pm 0.09$ and $a_f(\tau_w = 1) = 0.91 \pm 0.09$ for not-declustered and $a_f(\tau_u = 1) = 0.93 \pm 0.11$ and $a_f(\tau_w = 1) = 0.87 \pm 0.11$ for declustered. In all cases they are significantly larger than the expectance (0.5) of a random method with s.l.$\ll$0.01.

One question that may come to mind when looking at the results of such space-time analysis is how much of the observed forecasting performance is due to spatial clustering and how much to time clustering. In order to try to answer such question, we made some further computations in which the time clustering is eliminated by assuming in each CA a permanent alarm for the entire duration of the forecasting experiment (*T*=60 years). We computed the time-independent Molchan and AS score trajectories by adding step by step one CA at a time, starting from the CA with highest weight (highest long-term seismic activity) and then going on, up to add all CAs. At each step, the unweighted and weighted fractions of space occupied by alarms are computed by simply taking $\tau_c = 1$ in eq. (4) and (6) respectively for the included CAs and $\tau_c = 0$ for the not included CAs.

The results of such time-independent analysis for declustered (first) target shocks with Mw≥5.5 is shown in Figs. 7 and 8. Even if they are not fully comparable with the time-dependent analysis of Fig. 5 and 6 because the trajectories depend on the adopted ordering of the CAs, from the most to the least active, we can note that the skill of time-independent analysis appears definitely lower, particularly at small τ and for the weighted trajectories (blue lines). This can be easily explained by the higher time clustering at short times (and then at small τ) and by the fact that the weights based on the long-term seismic activity penalize more the CAs where the target shocks actually occurred in the last 60 years.

The results for declustered (first) target shocks with Mw≥5.0 and Mw≥6.0 are reported in Figs. S11, S12, S13 and S14 of supplemental material. For Mw≥5.0, the comparison of Fig. S11 and S12 with the time-dependent analysis of Figs. S5 and S6 is similar to the case for Mw≥5.5 described before.

For Mw≥6.0, the comparison of Fig. S13 and S14 with the time-dependent analysis of Figs. S9 and S10, apart for small τ, apparently indicates an overall higher skill for the time-independent analysis with respect to the time-dependent one. This is due to the fact that for Mw≥6.0 all declustered target shocks occurred in CAs with very high long-term seismic activity and that, as noted above, time-independent and time-dependent statistics are not fully comparable between them.

Optimization of the forecasting algorithm

For a practical application of the forecasting method, it might be useful to determine the values of the algorithm parameter Δt for which the forecasting method is more efficient and useful for risk mitigation. To accomplish this purpose, we analyse the behaviour of some statistics that depend on the alarm time window Δt.

In Fig. 9 we report, for declustered targets and weighted fraction of space-time occupied by alarms (τ_w), the binomial probability (Eq. 9), that is the probability that the observed number of successful forecasts is obtained by chance, as a function of Δt. The lower the probability the higher the strength of the forecast. In general, probabilities are relatively low within a wide range going from one day to some years. For Mw≥5.0 (red line), very low probabilities are observed around $\Delta t = 2 \div 10$ days. For Mw≥5.5 (blue line) and Mw≥6.0 (green line) the minimum probabilities are larger than the ones for Mw≥5.0, and they remain relatively low from a few hours to a few months. Within such ranges, the forecasting ability of our method reaches its higher efficiency.

The behaviour of the probability gain G (eq. 8) as a function Δt (Fig. 10) shows, for all the three magnitude thresholds, monotonically descending trends from more than 100000 at very short Δt (less than a minute) to slightly more than 1 at very long Δt (tens of years). Such curves also show relatively milder slopes in correspondence of steep decreases of binomial probabilities in Fig. 9 (i.e. around 0.001 day and a few days)

16

In Fig. 11 we show the miss rate ν as a function of Δt. In general, it decreases with increasing Δt. The (negative) trends - with respect to $\log_{10}\Delta t$ - are in between the -5% and -10% per decade, for Δt ranging from a few seconds to about 1 year. Then they start to decrease more rapidly (about -20% per decade) reaching 0 for Mw≥5.5 and Mw≥6.0 and 19% for Mw≥5.0 at very large Δt.

The behaviour of the same statistic for the full set of target events (not-declustered) is reported in Figs. S15, S16 and S17 of the supplemental material. It is similar to those of the declustered set but the binomial probabilities are lower, the probability gains are higher and the miss rates decrease more rapidly with Δt.

Another aspect to be considered for the practical application of the forecasting method is the dependence on Δt of the fractions of space-time occupied by alarms τ_u and τ_w (Fig. 12). A long alarm interval Δt (with a corresponding long fraction of space-time occupied by alarms τ) allows to forecast more target earthquakes but at the same time it has relatively lower probabilities of occurrence than a shorter Δt. Furthermore, a longer duration of alarms would impact more with life activities of the population in the involved area. Even if any decision on the possible practical application in real situations would eventually require a careful evaluation by decision makers even considering a cost-benefits analysis (e.g. van Stiphout et al., 2010, Hermann et al., 2016), we examine here as an example the choice of Δt= 3 months (0.25 years). This choice, in most cases, results in a fairly trade-off between a good efficiency and a narrow space-time fraction covered by alarms $\tau \approx$ 2.

We can see in Table 2 that in this case the method is able to retrospectively forecast more than 50% of not-declustered target shocks with Mw≥5.0 and more than 70% of those with Mw≥5.5 and Mw≥6.0. We also report in Table 2 the statistic of the numbers of successful alarms with respect to the total number of alarms indicating higher rates for target with Mw≥5.0. About one fifth of alarms actually forecast an earthquake, while the fraction of successful alarms definitely decreases for larger targets and further decreases for declustered sets down to about 1%. Note that several alarm time

windows are actually overlapped and then the total duration of alarms is shorter than the simple sum of alarm windows (Eq. 2).

The performance of the method is definitely worse for the first target shocks (declustered set) but it improves by increasing the magnitude of target shocks. Actually, 4 over 7 first target shocks with Mw≥6.0 over the last 60 years in Italy are retrospectively forecasted in this way.

We tested the stability with time of the forecasting performance by subdividing the seismic catalog in two equal parts of 30 years: before and after 1/1/1990. The same computations of Table 2 for Δt= 3 months for intervals 1960-1989 and 1990-2019 are reported in Tables 3 and 4 respectively. The rates of successfully forecasted target shocks (declustered or not) are similar in the two periods whereas the space-time fraction occupied by alarms is definitely lower in the most recent period, consistently with the higher ratios between successful and total alarms. We could argue that smaller magnitude errors in most recent times, owing to the continuous improvement of the Italian seismic network, reduce the amount of false alarms and then increase the observed skill of the forecasting method with respect to the previous period.

In Table 5 and 6 we report the lists of retrospective forecast of the first (declustered) target shocks with Mw≥5.5 and Mw≥6.0 respectively occurred in Italy from 1960 to 2019 (also see the results for the declustered first shocks with Mw≥5.0 in Table S8 and the results for not-declustered targets with Mw≥5.0, 5.5 and 6.0 in Tables S9, S10 and S11 respectively of the supplemental material).

We can note that for two target shocks (1976 Friuli and 1990 Potentino) the forecast could have hardly been used by civil protection services to adopt safety countermeasures because the forecasting strong shocks occurred too shortly before the main shock (67 s and 13 s respectively). In other cases, the time delay between the forecasting shock and the main shock (going from a couple of hours to a few weeks) would have been sufficient to take some countermeasures.

We could note that a foreshock did actually occur a couple of days before the first mainshock of 20 May 2012 (Mw=6.1) in the area of Pianura Emiliana but its magnitude (Mw=4.2) was only slightly below the lower threshold of Mw=4.4 we adopted. The retrospective ability to predict Mw≥6.0

18

earthquakes might have been improved then by slightly reducing such lower threshold but at a cost of a general reduction of the performance of the algorithm, because of the increment of the number of alarms and of the fraction of space-time covered by alarms.

Conclusions

We analysed a simple algorithm to forecast shallow (depth<50 km) main shocks (Mw≥5.0, 5.5, 6.0) that threaten the life and the goods of the population living on the Italian mainland territory, based on the previous occurrence within circular areas of 30 km of radius of widely felt strong shocks (4.4 ≤Mw<4.8) not particularly harmful in themselves. Based on a retrospective analysis of the HOmogenized instRUmental Seismic catalogue (HORUS) of Italy from 1960 to 2019 (Lolli et al., 2020) this method retrospectively forecast the majority of damaging earthquakes occurred in Italy in the past 60 years by issuing alarms covering only a small fraction of the space-time coverage.

We estimated such fraction even considering the different levels of seismic activity in different areas of Italy by weighting more the alarm times in circular areas where the average seismicity rate, computed from the CPTI15 seismic catalogue (Rovida et al., 2016, 2020) from 1600 to 1959, is higher.

The retrospective testing using the Molchan diagram (Molchan, 1990, 1991, Molchan & Kagan, 1992) and the Area Skill score (Zechar & Jordan, 2008) methods indicates that such approach clearly overperforms a purely random method with high or very high confidence, depending on the target shock magnitude threshold.

As the secondary main shocks during seismic sequences are definitely easier to be forecasted by this method because the aftershocks of the first main shock usually generate alarms at weakly (if not daily) rate, we also tested the ability of our approach to predict only the first main shock of each sequence. We found that the forecasting ability remains high even if being lower than that considering all main shocks.

Even if the true verification of the efficiency of the method will only be made on a prospective dataset, we believe that such simple forecasting algorithm could be useful, like other operational forecasting approaches presently considered by the Italian Civil Protection Department, for planning preparation measures in the field (e.g. Marzocchi et al., 2014).

The latter approaches are mainly based on the ETAS model (Kagan & Knopoff, 1987, Ogata, 1988) and, as well as that of the present work, showed to retrospectively forecast the evolution of Italian seismicity better than an inhomogeneous random process with spatial rates corresponding to past seismicity. On the other hand, Marzocchi and Zhuang (2011) showed that ETAS models is able to describe quite well even the observed foreshock activity. However, a comparison of the relative efficiency of our approach with ETAS models and even with other forecasting approaches (like for example the EEPAS method (Rhoades and Evison, 2004) would require that the probabilistic formulation of the latter methods is adapted to the alarm-based one (for example by selecting a particular probability thresholds above which to declare an alarm). However, such adaptation is not trivial and hence, the question on which of the different approaches is better in predicting future damaging earthquakes remains not answered presently and has to be deferred to future papers comparing all methods in an alarm-based context by using, for example, the approach proposed by Shebalin et al. (2014).

One advantage of the present forecasting approach is that it is easy to implement and communicate because it does not require any other scientific analysis than the correct determination of the location and of the magnitude of the precursory shock. In principle every person could be informed very quickly by a notification sent by one of the already available mobile Apps which provide near real-time access to the INGV online earthquake list (http://terremoti.ingv.it/en#).

Acknowledgements

References

Agnew, D.C. & Jones, L.M., 1991. Prediction probabilities from foreshocks, *J. geophys. Res.*, **96**, 11 959–11 971.

Caputo, M., Gasperini, P., Keilis-Borok, V., Marcelli, L. & Rotwain, I., 1977. Earthquakes swarms as forerunners of strong earthquakes in Italy, Annali di Geofisica, 30, 269-283, doi: 10.4401/ag-4823.

Caputo, M., Console, R., Gabrielov, A.M., Keilis-Borok, V.I & Sidorenko, T.V., 1983. Long-term premonitory seismicity patterns in Italy, Geophys. J. R. astr. Soc., 75, 71-75.

Console, R., Murru, M. & Alessandrini, B., 1993. Foreshock statistics and their possible relationship to earthquake prediction in the Italian region, Bull. Seism. Soc. Am., 83, 4, 1248-1263.

Console, R. & Murru, M., 1996. Probability gain due to foreshock following quiescence tested by synthetic catalogs, Bull. Seism. Soc. Am., 86, No. 3, 911-913.

Console, R & Murru, M., 2001. A simple and testable model for earthquake clustering, J. Geophys. Res., 106, 8699- 8711, doi:10.1029/2000JB900269.

Console, R., Di Luccio, F., Murru, M., Imoto, M. & Stavrakakis, G., 1999. Short Term and Short Range Seismicity Patterns in Different Seismic Areas of the World, Natural Hazard, 19, 107-121.

Console, R, Murru, M & Lombardi, A. M., 2003. Refining earthquake clustering models, J. Geophys. Res ., 108:2468, doi:10.1029/2002JB002130.

Console, R, Murru, M & Catalli, F., 2006. Physical and stochastic models of earthquake clustering, Tectonophysics, 417, 141–153, doi: 10.1016/j.tecto.2005.05.052.

Di Luccio, F., Console., R., Imoto, M. & Murru, M., 1997. Analysis of short time-space range seismicity patterns in Italy, Annali di Geofisica, 40/4, 783-798.

Gardner, J.K. & Knopoff, L., 1974. Is the sequence of earthquakes in Southern California, with aftershocks removed, Poissonian? Bull. Seism. Soc. Am., 64, 1363-1367.

Gasperini, P., Lolli, B., Vannucci, G., Boschi, E., 2012. A comparison of moment magnitude estimates for the European–Mediterranean and Italian region, Geophys. J. Int., 190, 1733-1745, doi: 10.1111/j.1365-246X.2012.05575.x.

Gasperini P., Lolli, B. & Vannucci, G., 2013. Empirical Calibration of Local Magnitude Data Sets Versus Moment Magnitude in Italy, Bull., Seism. Soc. Am., 103, 2227-2246, doi: 10.1785/0120120356.

Gasperini P., Lolli, B. & Vannucci, G., 2016. Relative frequencies of seismic main shocks after strong shocks in Italy, Geophys. J. Int., 207, 150-159, doi: 10.1093/gji/ggw263.

Geller, R., Jackson, D.D., Kagan, Y.Y. & Mulargia, F., 1997. Earthquakes cannot be predicted, Science, 275, 1661, doi: 10.1126/science.275.5306.1616.

Gutenberg, B., & Richter, C.F., 1944. Frequency of earthquakes in California, Bull. Seism. Soc. Am., 34: 185-188.

Grandori, G., Guagenti, E. & Perotti, F., 1988. Alarm systems based on a pair of short-term earthquake precursors, Bull. Seism. Soc. Am., 78, no. 4, 1538-1549.

Hermann, M., Zechar, J.D. & Wiemer, S., 2016. Communicating time-varying seismic risk during an earthquake sequence, Seism. Res. Lett., 87, 2A, 30-312, doi: 10.1785/0220150168.

Jones, L.M., 1984. Foreshocks (1966–1980) in the San Andreas system, California, Bull. seism. Soc. Am., 74, 1361–1380.

Jones, L.M., 1985. Foreshocks and time-dependent earthquake hazard assessment in southern California, Bull. seism. Soc. Am., 75, 1669–1680.

Jones, L.M., 1994. Foreshocks, aftershocks, and earthquake probabilities accounting for the Landers earthquake, Bull. Seism. Soc. Am., 84, no. 1, 892-899.

Jones, L. & Molnar, P. , 1976. Frequency of fore- shocks, Nature, 262., 677-679, 1976.

Jones, L. & Molnar, P., 197. Some characteristics of foreshocks and their possible relationship to earthquake prediction and premonitory slip on faults, J. Geophys. Res., 84, B7, 3596-3608.

Jordan, T.H., 2006. Earthquake predictability, brick by brick, Seismol. Res. Lett., 77(1), 3–6.

Jordan, T.H., Chen, Y., Madariaga, R., Main, I.., Marzocchi, W., Papadopulos, G., Sobolev, G., Yamaoka, K. & Zschau, J., 2011. Operational earthquake forecasting: state of knowledge and guidelines for implementation, final report of the international commission on earthquake forecasting for civil protection, *Ann. Geophys.*, **54**(4), 315–391.

Jordan, T.H. & Jones, L.M., 2010. Operational earthquake forecasting: some thoughts in why and how, Seism. Res. Lett., 81/4, 571-574, doi: 10.1785/gssrl.81.4.571.

Kagan, Y.Y., 2014. Earthquakes, AGU-Wiley, 283 pp.

Kagan, Y., & Knopoff, L. 1987. Statistical short-term earthquake prediction, Science 236, 1563–1567.

Lolli, B., Gasperini, P. & Rebez, A., 2018. Homogenization in terms of Mw of local magnitudes of Italian earthquakes occurred before 1981, Bull. Seism. Soc. Am., 108, No. 1, 481–492, doi: 10.1785/0120170114.

Lolli, B., Randazzo, D., Vannucci, G. & Gasperini, P., 2020, HOmogenized instRUmental Seismic catalog (HORUS) of Italy from 1960 to present, Seism. Res. Lett. 91, 3208-3222, doi: 10.1785/0220200148.

Marzocchi, W., Lombardi, A. M. & Casarotti, E., 2014. The Establishment of an Operational Earthquake Forecasting System in Italy, Seism. Res. Lett., 85/5, 961-969, doi: 10.1785/0220130219.

Marzocchi, W. & Zhuang, J., 2011. Statistics between mainshocks and foreshocks in Italy and Southern California, Geophys. Res. Lett., 38, L09310, doi:10.1029/2011GL047165.

Molchan, G. M.,1990. Strategies in strong earthquake prediction, Phys. Earth and Planet. Inter. 61, 84–98.

Molchan, G.M., 1991. Structure of optimal strategies in earth- quake prediction, Tectonophys. 193, 267–276.

Molchan, G. M. & Kagan, Y. Y., 1992, Earthquake predictionand its optimization, J. Geophys. Res. 97, 4823–4838.

Mulargia, F. & Geller, R.J., 2003. Earthquake Science and Seismic Risk Reduction, Kluwer, 338 pp.

Ogata, Y. 1988. Statistical models for earthquake occurrences and residual analysis for point processes, J. Am. Stat. Assoc. 83, 9–27.

Reasenberg, P.A., 1985. Second-order moment of central California seismicity, 1969-1982, J. Geophys. Res., 90: 5479-5495.

Reasenberg P.A., 1999a. Foreshock occurrence before large earthquakes, J. Geophys. Res., 104, B3, 4755-4768.

Reasenberg, P.A., 1999b. Foreshock occurrence rates before large earthquakes worldwide, Pure Appl., Geophys., 155, 355-379.

Rhoades, D. A. and Evison, F. F. (2004). Long-range earthquake forecasting with every earthquake a precursor according to scale. Pure and Applied Geophysics, 161:47–72.

Rovida, A., Locati, M., Camassi, R., Lolli, B. & Gasperini, P., 2016. CPTI15. The 2015 Version of the Parametric Catalogue of Italian Earthquakes, Istituto Nazionale di Geofisica e Vulcanologia, doi: 10.6092/INGV.IT-CPTI15.

Rovida, A., Locati, M., Camassi, R., Lolli, B. & Gasperini, P., 2020. The Italian earthquake catalogue CPTI15, Bull. Earth. Eng., 18, 2953-2984, doi: 10.1007/s10518-020-00818-y.

Schorlemmer, D., Christophersen, A., Rovida, A., Mele, F., Stucchi, M. & Marzocchi, W., 2010. Setting up an earthquake forecast experiment in Italy, Annals of Geophysics, 53/3, 1-9, doi: 10.4401/ag-4844.

Southern San Andreas Working Group (1991). Short-Term Earthquake Hazard Assessment for the San Andreas Fault in Southern California, U.S. Geological Survey, Open-file Report 91-31.

Shebalin, P., Narteau, C., Holschneider, M. & Schorlemmer, D., 2011. Short-Term Earthquake Forecasting Using Early Aftershock Statistics, Bull. Seism. Soc. Am., 101, 297-312, doi: 10.1785/0120100119.

Shebalin, P., Narteau, C., Zechar, J. D. & Holschneider, M., 2014. Combining earthquake forecasts using differential probability gains, Earth, Planets and Space, 66:37, doi: 10.1186/1880-5981-66-37.

van Stiphout, T., Wiemer, S. & Marzocchi, W., 2010. Are short-term evacuations warranted? Case of the 2009 L'Aquila earthquake, Geophys. Res. Lett. 37, no. 6, 1–5, doi: 10.1029/2009GL042352.

Zechar J. D. & Jordan, T. H., 2008. Testing alarm-based earthquake predictions, Geophys. J. Int. 172, 715–724 doi: 10.1111/j.1365-246X.2007.03676.x.

Zechar J. D. & Jordan, T. H., 2010. The Area Skill Score Statistic for Evaluating Earthquake Predictability Experiments, Pure Appl. Geophys. 167, 893–906, doi:10.1007/s00024-010-0086-0.

Zechar, J. D., Schorlemmer, D., Liukis, M., Yu, J., Euchner, F., Maechling, P. J., Jordan, T. H., 2010. The Collaboratory for the Study of Earthquake Predictability perspective on computational earthquake science. Concurr. Comput. 22, 1836–1847, doi: 10.1002/cpe.151

Figures
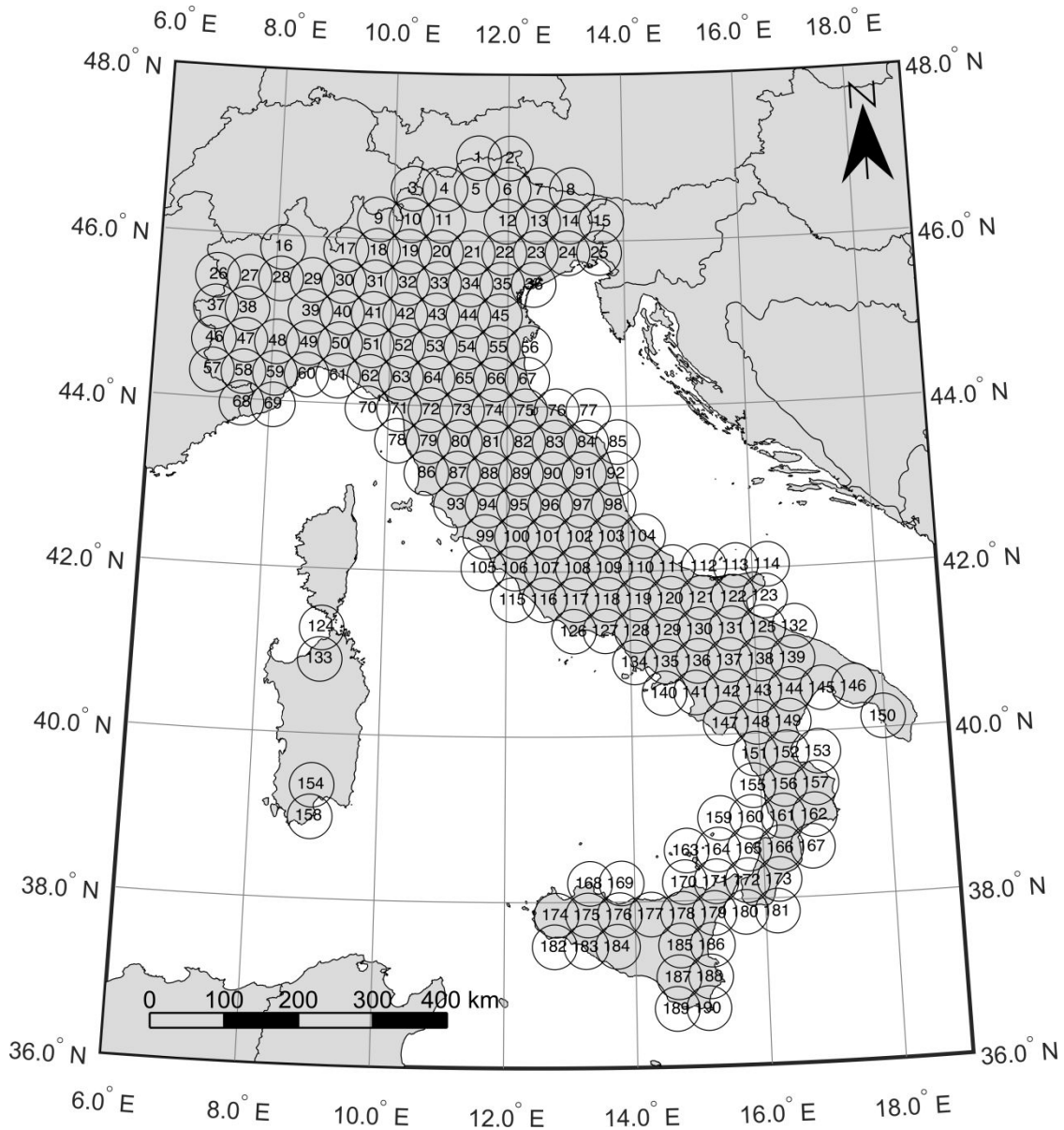
Figure 1- Tessellation of the Italian territory used for the retrospective forecast experiment. Circular areas (CA) with R=30 km within which at least one earthquake with Mw≥4.0 occurred inland from 1600 to 1959 according to the CPTI15 catalogue (Rovida et al., 2020).
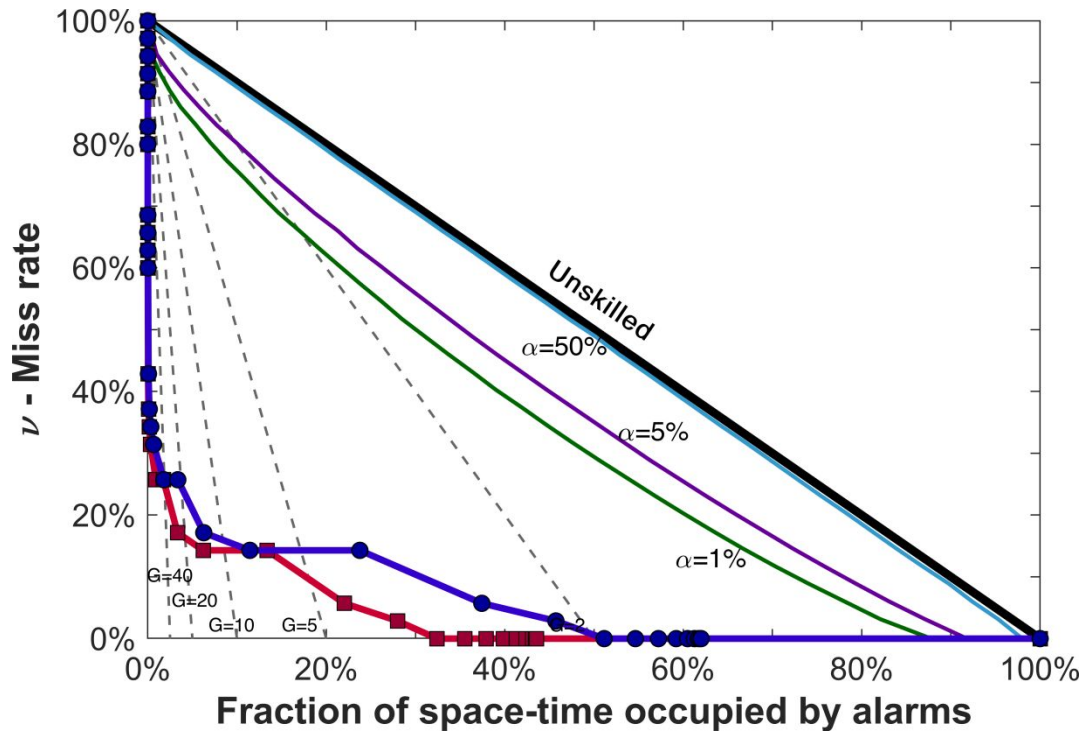
Figure 2 – Molchan diagram for all target shocks with Mw≥5.5 (not-declustered). Red and dark blue lines indicate the forecasting performance of foreshocks with 4.4≤Mw<4.8 for unweighted (τ_u) and weighted (τ_w) fractions of space-time occupied by alarms respectively (see text). The black continuous line indicates a purely random forecasting method that separates skilled (below the line) from unskilled (above) forecasting methods. The light blue, violet and green lines indicate the confidence limits for α =50%, 5% and 1% respectively. The black dashed lines indicate probability gains G=2, 5, 10, 20 and 50.
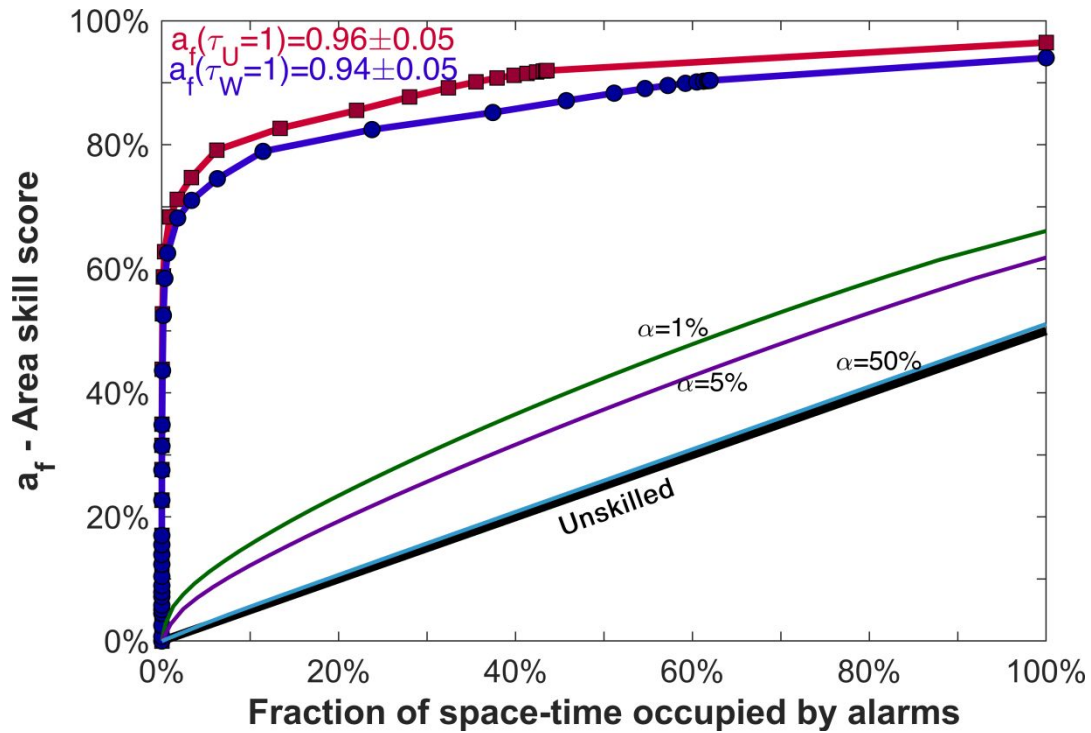
Figure 3 – Area skill score diagram for all target shocks with Mw≥5.5 (not-declustered). Red and dark blue lines indicate the forecasting performance of foreshocks with 4.4≤Mw<4.8 for unweighted (τ_u) and weighted (τ_w) fractions of space-time occupied by alarms respectively (see text). The black continuous line indicates the performance of a purely random forecasting method that separates skilled (below the line) from unskilled (above) forecasting methods. The light blue, violet and green lines indicate the confidence limits for α =50%, 5% and 1% respectively.
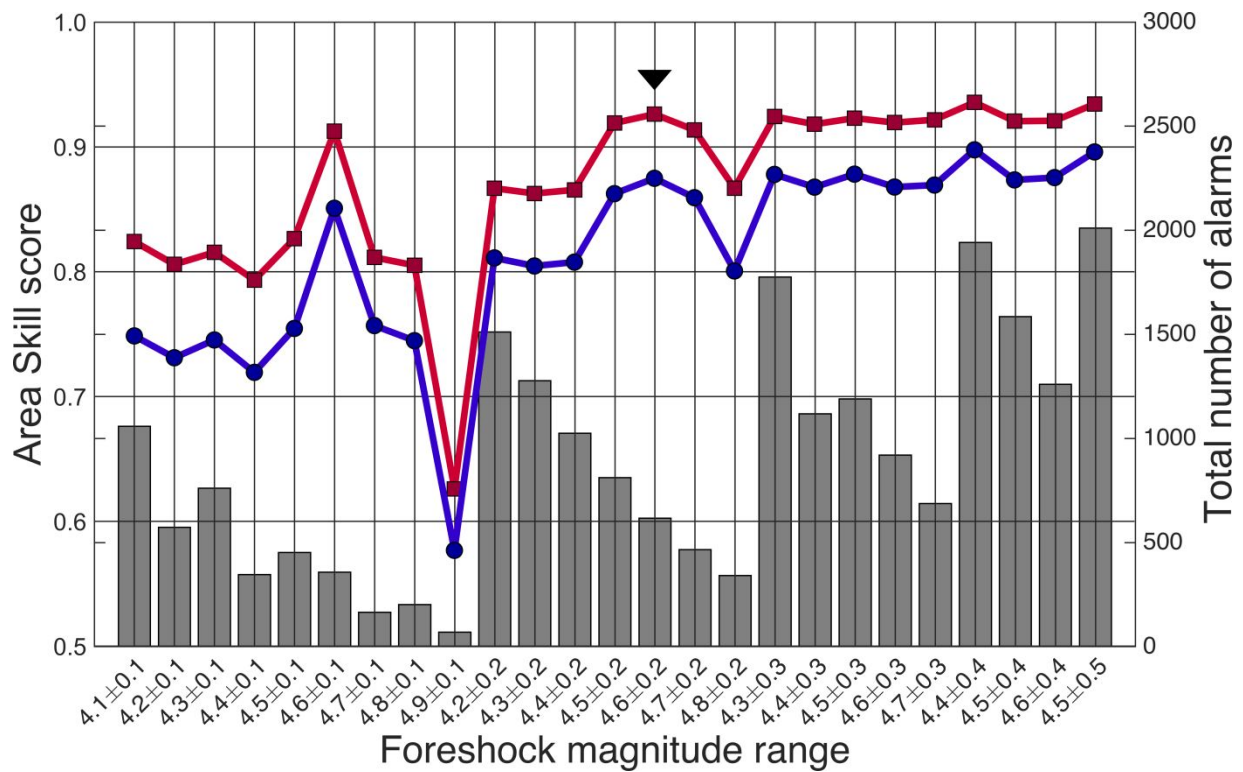
Figure 4 – Area Skill (AS) score computed for declustered targets with Mw≥5.5, using unweighted (red line) and weighted (blue) fractions of space-time occupied by alarms, and total number of alarms (grey bars) as a function of the foreshock magnitude range. The arrows indicate the range Mw=4.6±0.2, chosen as best compromise between high AS score and low number of alarms.
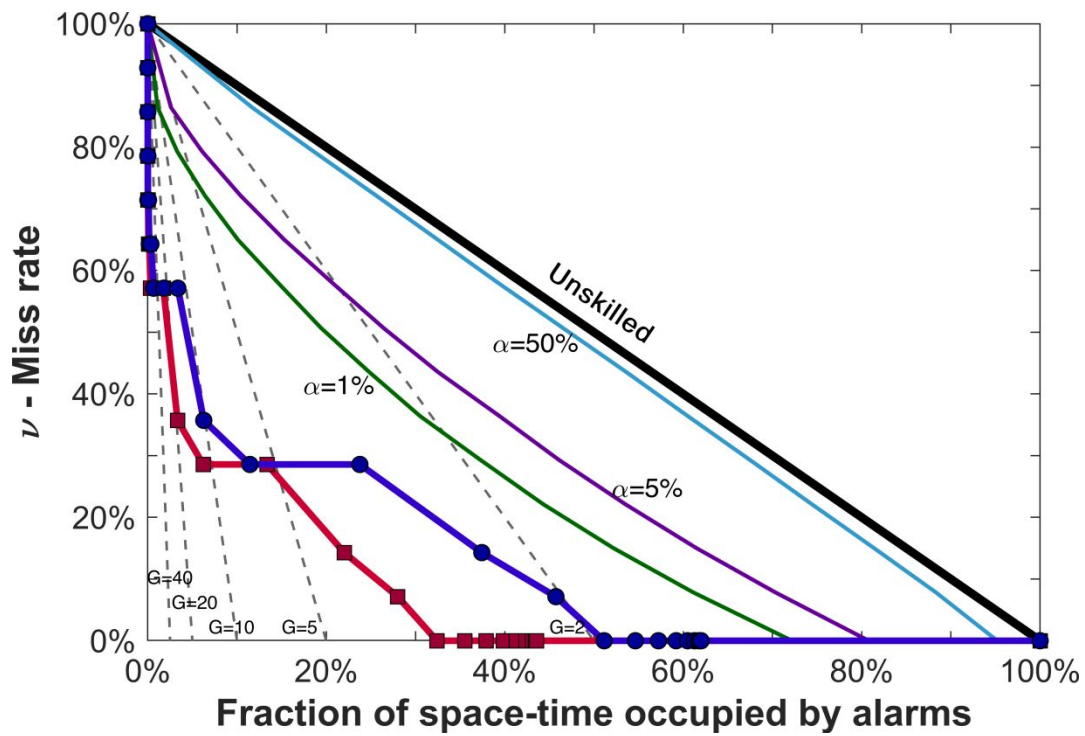
Figure 5 – Same as Fig. 2 for declustered (first) target shocks with Mw≥5.5.
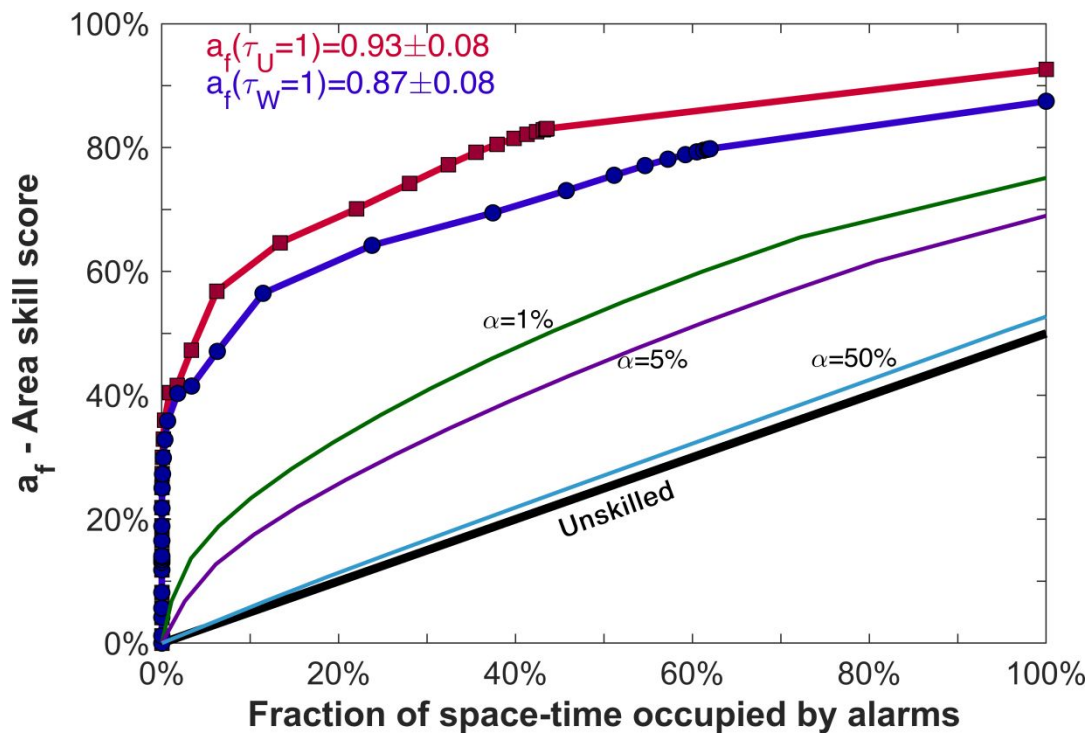
Figure 6 – Same as Fig. 3 for declustered (first) target shocks with Mw≥5.5.
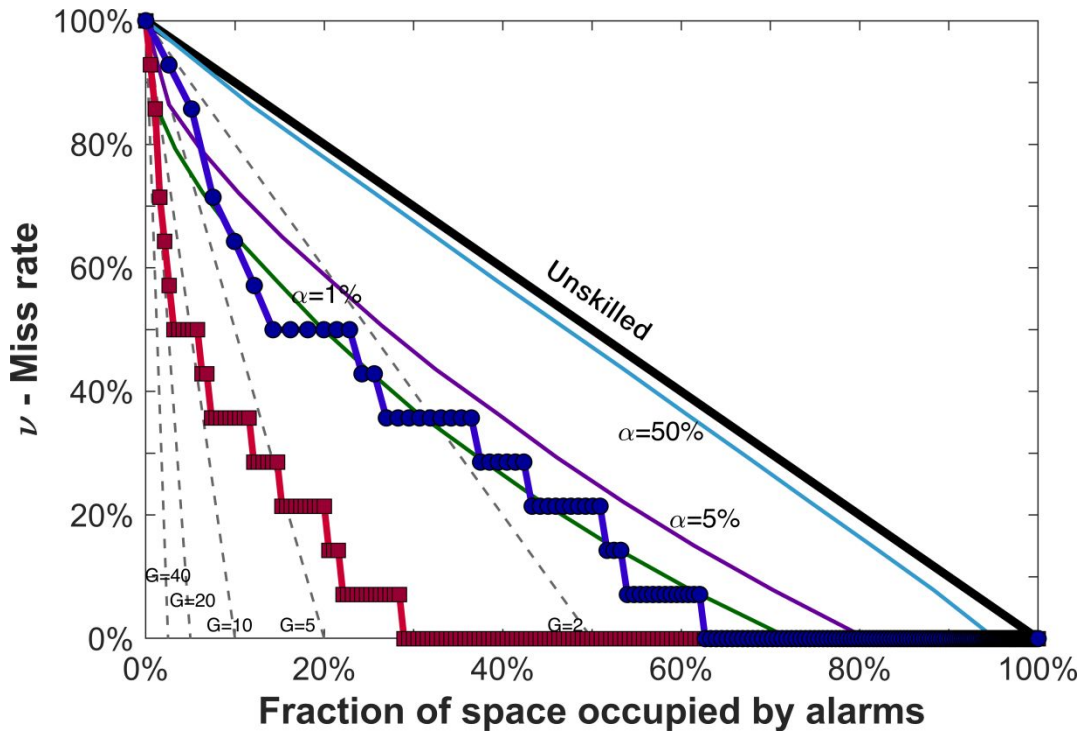
Figure 7 – Same as Fig. 2 for time-independent analysis of declustered (first) target shocks with Mw≥5.5.
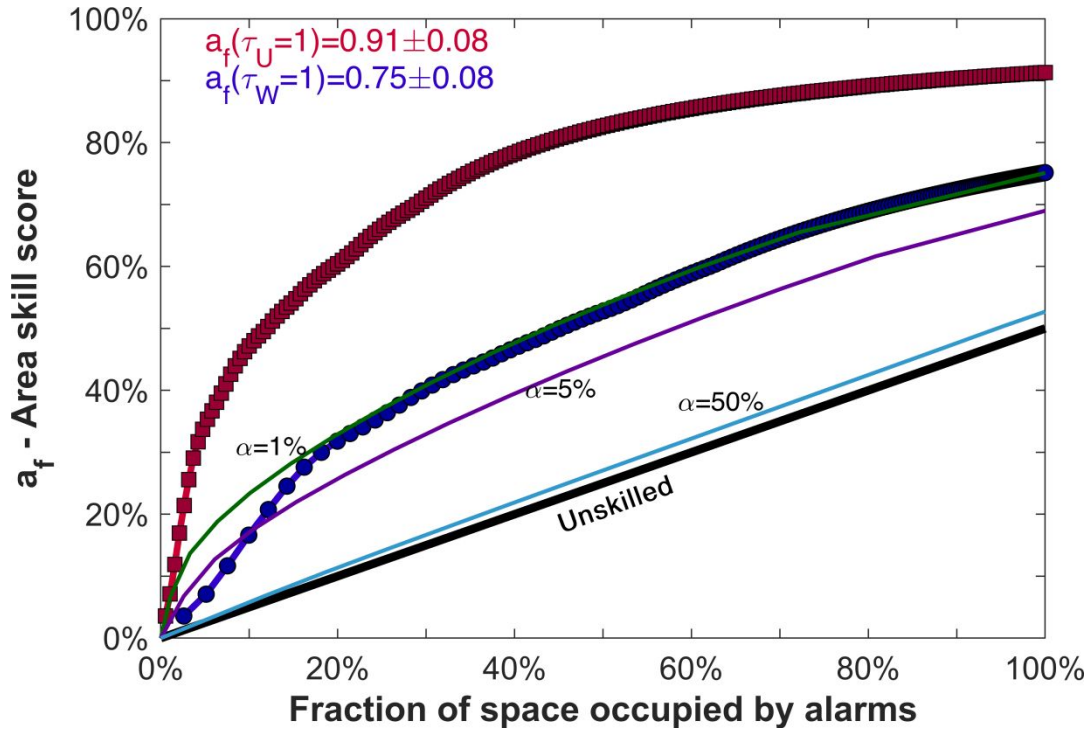
Figure 8 – Same as Fig. 3 for time-independent analysis of declustered (first) target shocks with Mw≥5.5.
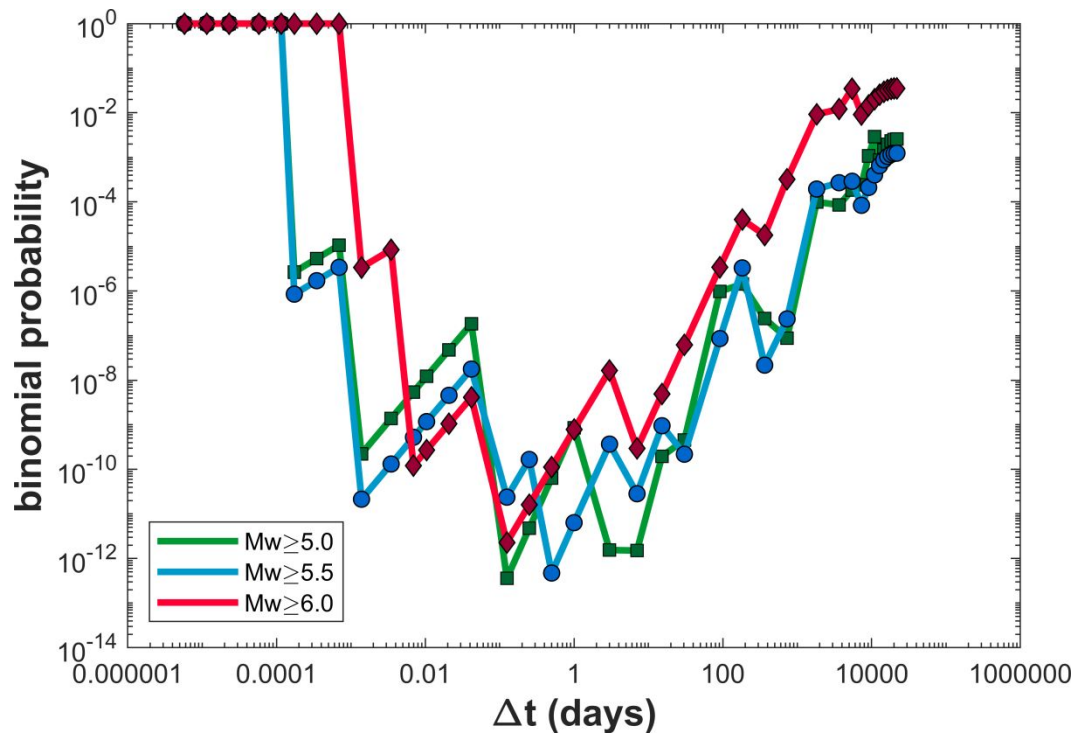
Figure 9 – Binomial probability density for declustered (first) target shocks and weighted fraction of space-time occupied by alarms for different magnitude thresholds (see inset) as a function of the alarm duration Δt.
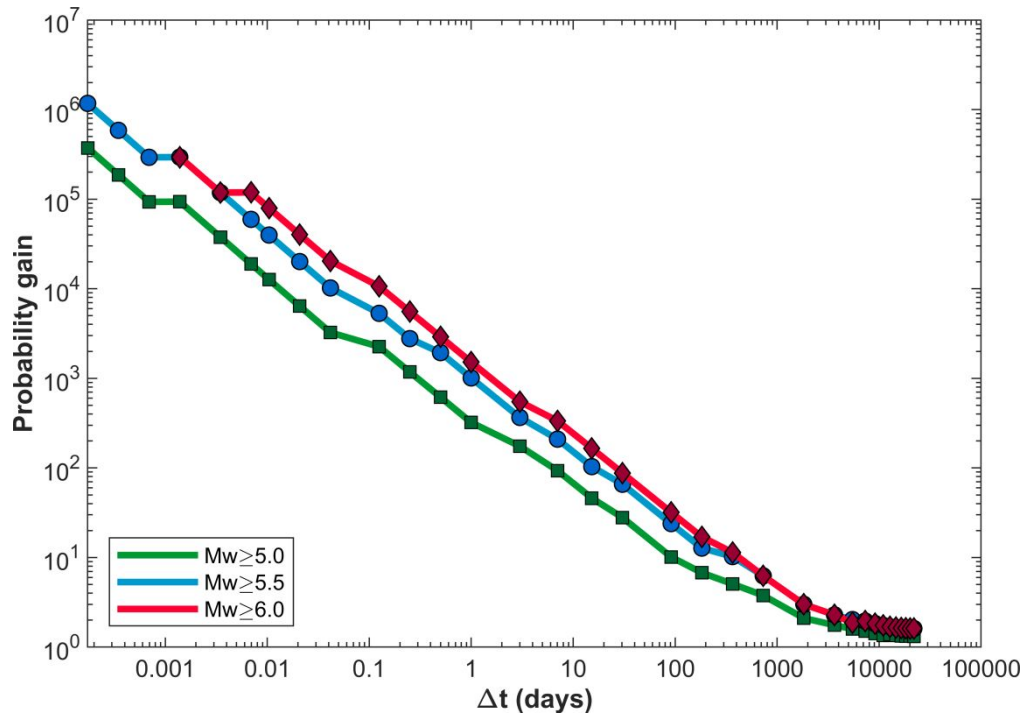
Figure 10 – Probability gain for declustered (first) target shocks and weighted fraction of space-time occupied by alarms for different magnitude thresholds (see inset) as a function of the alarm duration Δt.

Figure 11 – Miss rate for declustered (first) target shocks and different magnitude thresholds (see inset) as a function of the alarm duration Δt.
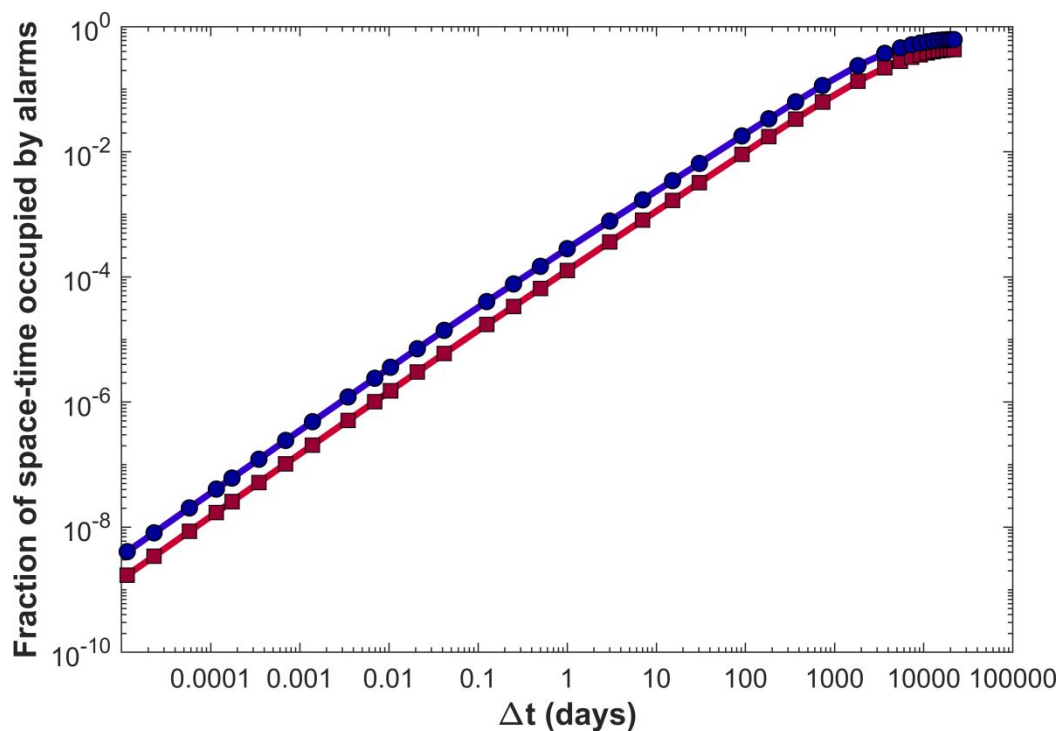
Figure 12 – Unweighted (red) and weighted (dark blue) fraction of space-time occupied by alarms as a function of the alarm duration Δt.

Tables

Table 1 – Magnitudes of completeness of the CPTI15 catalogue (Rovida et al., 2016, 2020)

Magnitude threshold Mc	Time interval of completeness	ΔT (years)
Mw≥4.5	1880-1959	80
Mw≥5.0	1880-1959	80
Mw≥5.5	1780-1959	180
Mw≥6.0	1620-1959	340

Table 2 – Retrospective forecasting performance of the algorithm for Δt= 3 months.

Target Magnitude	≥ 5.0		≥ 5.5		≥ 6.0		τ_u	τ_w
			Not-declustered					
Forecasted/total shocks	55/98	56%	26/35	74%	7/10	70%	0.9%	1.9%
Successful/total alarms	115/617	18.6%	72/617	11.7%	30/617	4.9%	0.9%	1.9%
			Declustered					
Forecasted/total shocks	8/44	18%	6/14	43%	4/7	57%	0.9%	1.9%
Successful /total alarms	13/617	2.1%	9/617	1.5%	8/617	1.3%	0.9%	1.9%

Table 3 – Same as Table 2 for the time interval 1960-1989.

Target Magnitude	≥ 5.0		≥ 5.5		≥ 6.0		τ_u	τ_w
			Not-declustered					
Forecasted/total shocks	21/45	47%	11/15	73%	3/4	75%	1.0%	2.1%
Successful/total alarms	45/336	12.9%	22/336	6.6%	9/336	2.7%	1.0%	2.1%
			Declustered					
Forecasted/total shocks	3/25	12%	3/7	43%	2/3	67%	1.0%	2.1%
Successful/total alarms	5/336	1.5%	5/336	1.5%	3/336	0.89%	1.0%	2.1%

Table 4 – Same as Table 2 for the time interval 1990-2019.

Target Magnitude	≥ 5.0		≥ 5.5		≥ 6.0		τ_u	τ_w
			Not-declustered					
Forecasted/total shocks	34/53	64%	15/20	75%	4/6	67%	0.4%	0.7%
Successful/total alarms	70/281	24.9%	50/281	17.8%	21/281	7.5%	0.4%	0.7%
			Declustered					
Forecasted/total shocks	5/19	26%	3/7	43%	2/4	50%	0.4%	0.7%
Successful/total alarms	8/281	3.5%	4/281	1.4%	5/281	1.8%	0.4%	0.7%

Table 5 – Results of retrospective forecast of first main shocks (declustered targets) with Mw≥5.5 in Italy from 1960 to 2019, using Δt= 3 months (0.25 years).

Year	Month	Day	Lat	Lon	Mw	t_a (days)		Epicentral area
1962	8	21	41.233	14.933	5.7	0.093	2.22 h	Irpinia
1968	1	15	37.700	13.100	5.7	0.425	10.2 h	Valle del Belice
1976	5	6	46.250	13.250	6.5	7.8×10^{-4}	67 s	Friuli
1979	*9*	*19*	*42.717*	*12.950*	*5.8*	*Missed*		*Valnerina*
1980	*11*	*23*	*40.800*	*15.367*	*6.8*	*Missed*		*Irpinia-Basilicata*
1984	*4*	*29*	*43.204*	*12.585*	*5.6*	*Missed*		*Umbria settentrionale*
1984	*5*	*7*	*41.666*	*13.820*	*5.9*	*Missed*		*Monti della Meta*
1990	5	5	40.650	15.882	5.8	1.5×10^{-4}	13 s	Potentino
1997	9	26	43.023	12.891	5.7	22.1		Appennino umbro-marchigiano
1998	*9*	*9*	*40.060*	*15.949*	*5.5*	*Missed*		*Appennino lucano*
2002	*10*	*31*	*41.717*	*14.893*	*5.7*	*Missed*		*Molise*
2009	4	6	42.342	13.380	6.3	6.5		Aquilano
2012	*5*	*20*	*44.896*	*11.264*	*6.1*	*Missed*		*Pianura Emiliana*
2016	*8*	*24*	*42.698*	*13.234*	*6.2*	*Missed*		*Monti della Laga*

t_a is the maximum time advance of the foreshock with respect to the main shock. "*Missed*" indicates that the target shock was not forecasted. Epicentral area identifiers are taken from the CPTI15 catalogue (Rovida et al., 2016, 2020).

Table 6 – Same as Table 2 for first main shocks with Mw≥6.0.

Year	Month	Day	Lat	Lon	Mw	t_a (days)		Epicentral area
1962	8	21	41.233	14.933	6.2	0.100	2.40 h	Irpinia
1976	5	6	46.250	13.250	6.5	7.8×10^{-4}	67 s	Friuli
1980	*11*	*23*	*40.800*	*15.367*	*6.8*	*Missed*		*Irpinia-Basilicata*
1997	9	26	43.015	12.854	6.0	22.5		Appennino umbro-marchigiano
2009	4	6	42.342	13.380	6.3	6.5		Aquilano
2012	*5*	*20*	*44.896*	*11.264*	*6.1*	*Missed*		*Pianura Emiliana*
2016	*8*	*24*	*42.698*	*13.234*	*6.2*	*Missed*		*Monti della Laga*

Retrospective short-term forecasting experiment in Italy based on the occurrence strong (fore) shocks

Supplemental material

P. Gasperini[1,2], E. Biondini[1], B. Lolli[2], A. Petruccelli[1,3], G. Vannucci[2]

[1]Dipartimento di Fisica e Astronomia, Università di Bologna, Italy

[2]Istituto Nazionale di Geofisica e Vulcanologia, Sezione di Bologna, Italy

[3] Swiss Seismological Service, ETH Zurich, Switzerland

paolo.gasperini@unibo.it, emanuele.biondini2@unibo.it, barbara.lolli@ingv.it,

antonio.petruccelli@sed.ethz.ch, gianfranco.vannucci@ingv.it

1
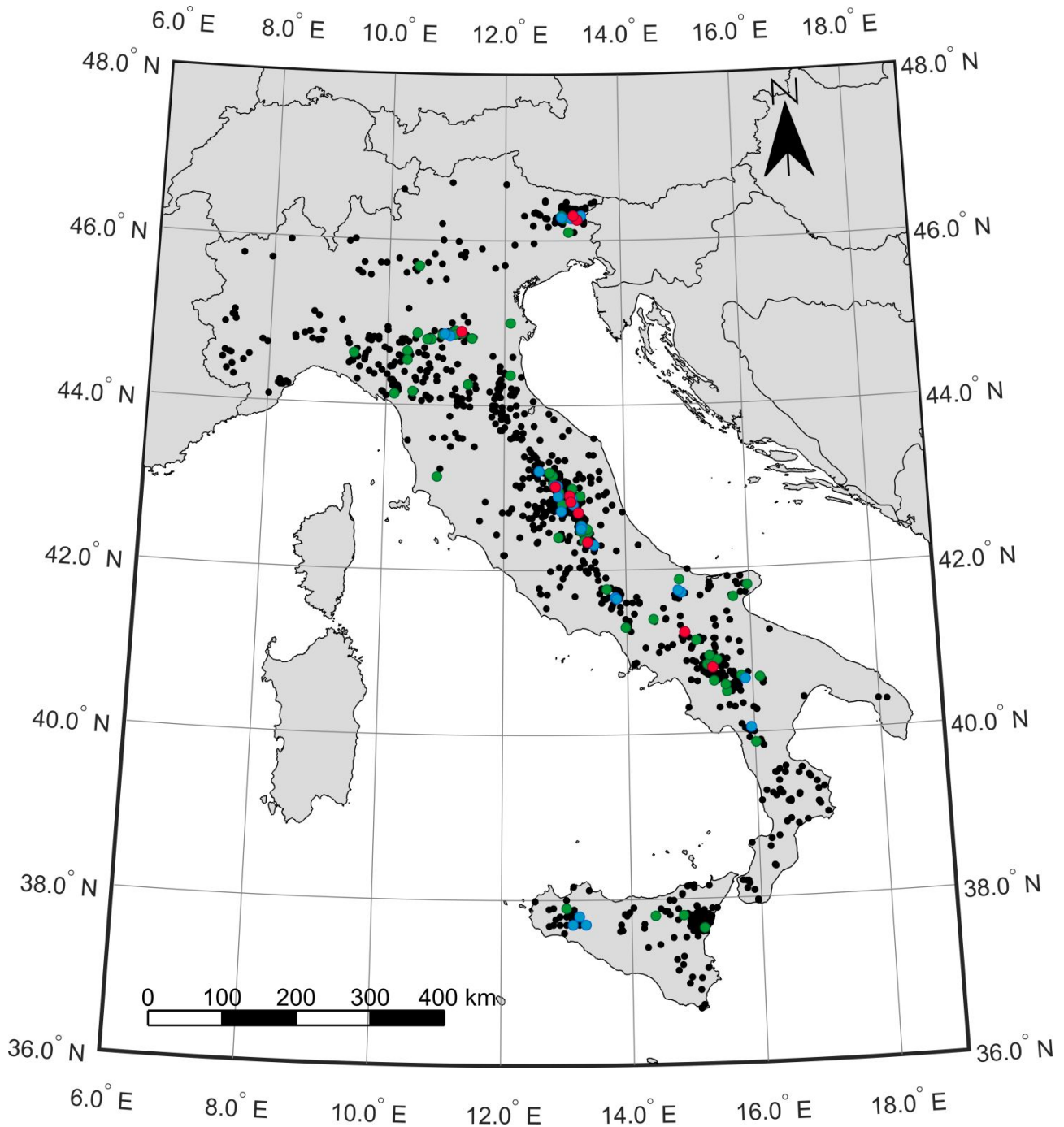
Figure S1 – Spatial distribution of inland earthquakes from the HORUS catalogue (Lolli et al., 2020) with Mw≥4.0 and depth <50 km used for testing and optimization. Black dots indicate 4.0≤Mw<5.0, green dots 5.0≤Mw<5.5, blue dots 5.5≤Mw<6.0, red dots Mw≥6.0.
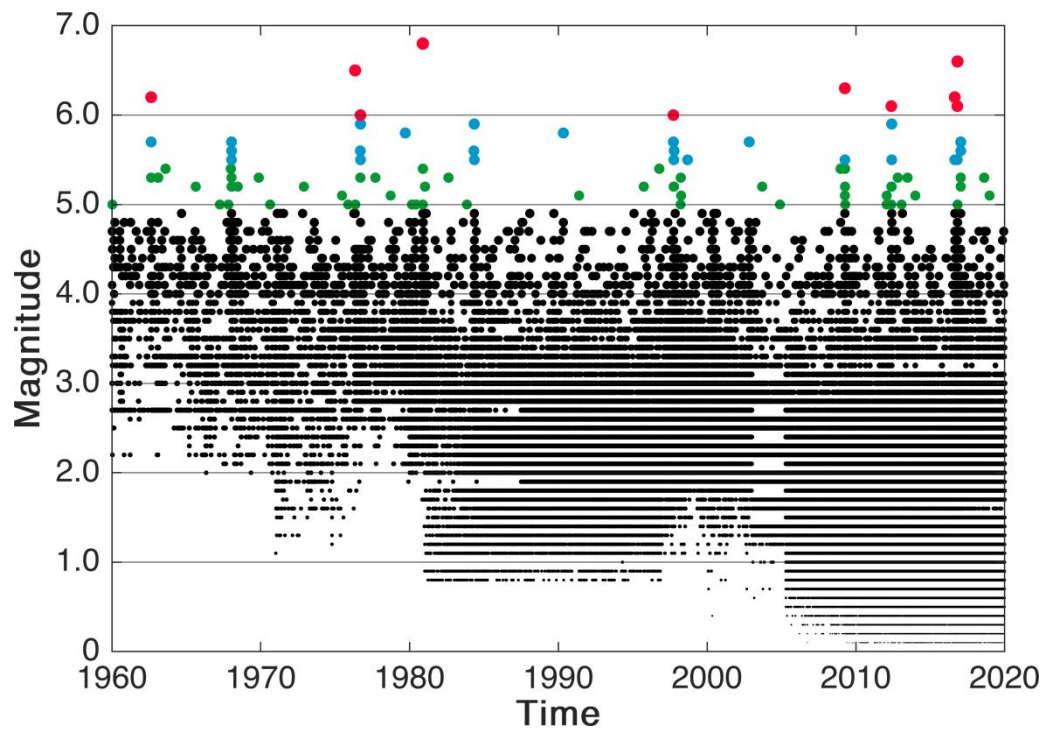
Figure S2 – Time distribution of magnitudes of inland earthquakes km from the HORUS catalogue (Lolli et al., 2020) with depth <50 km used for testing and optimization. Black dots indicate Mw<5.0, green dots 5.0≤Mw<5.5, blue dots 5.5≤Mw<6.0, red dots Mw≥6.0.
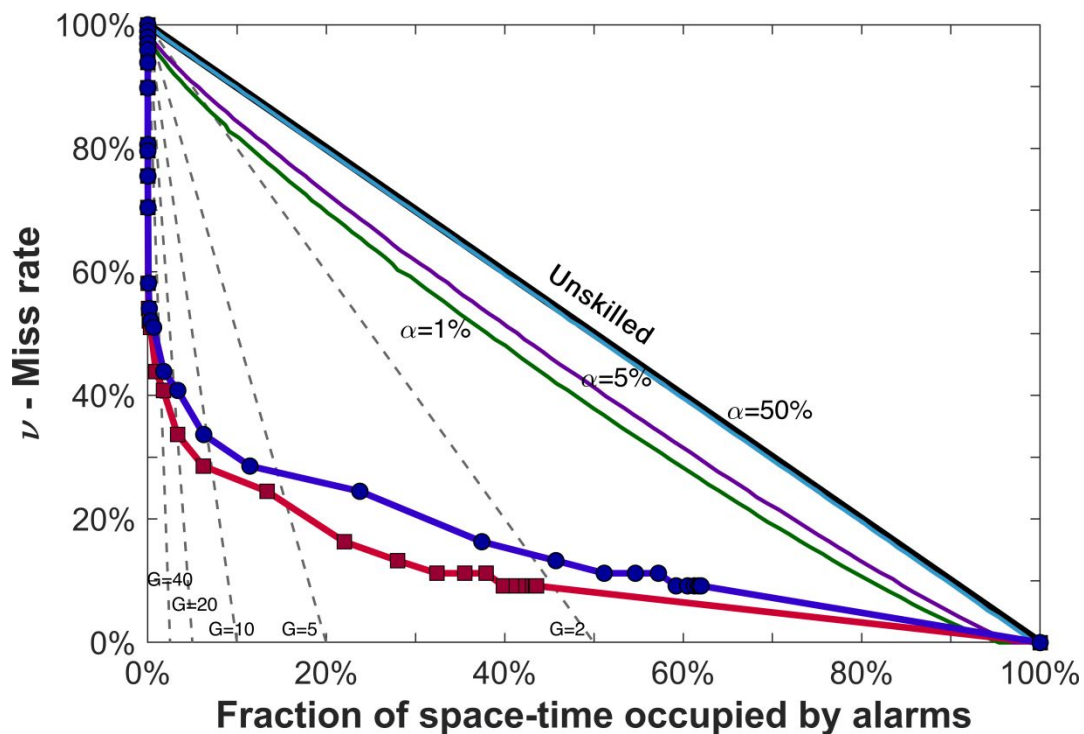
Figure S3 – Molchan diagram for all target shocks with Mw≥5.0 (not-declustered). Red and dark blue lines indicate the forecasting performance of foreshocks with 4.4≤Mw<4.8 for unweighted (τ_u) and weighted (τ_w) fractions of space-time occupied by alarms respectively (see main text). The black continuous line indicates the performance of a purely random forecasting method that separates skilled (below the line) from unskilled (above) forecasting methods. The light blue, violet and green lines indicate the confidence limits for α =50%, 5% and 1% respectively. The black dashed lines indicate probability gains G=2, 5, 10, 20 and 50.

Figure S4 – Area skill score diagram for all target shocks with Mw≥5.0 (not-declustered). Red and dark blue lines indicate the forecasting performance of foreshocks with 4.4≤Mw<4.8 for unweighted (τ_u) and weighted (τ_w) fractions of space-time occupied by alarms respectively (see main text). The black continuous line indicates the performance of a purely random forecasting method that separates skilled (below the line) from unskilled (above) forecasting methods. The light blue, violet and green lines indicate the confidence limits for α =50%, 5% and 1% respectively.
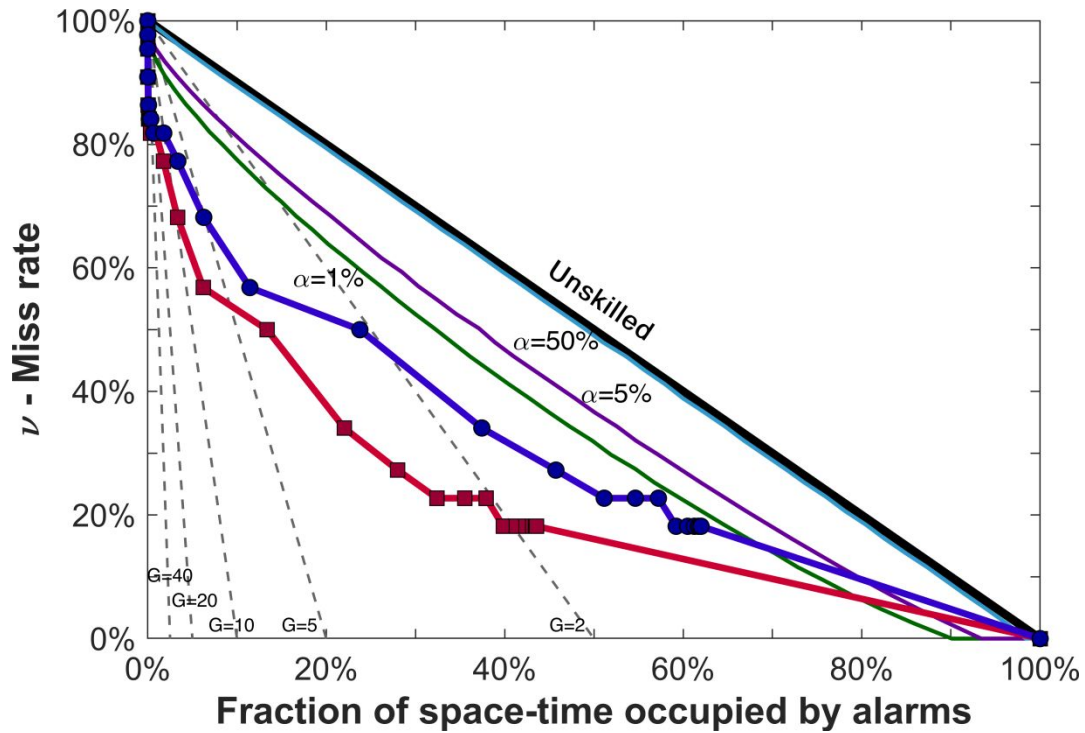
Figure S5 – Same as Fig. S2 for declustered (first) target shocks with Mw≥5.0 (see text).
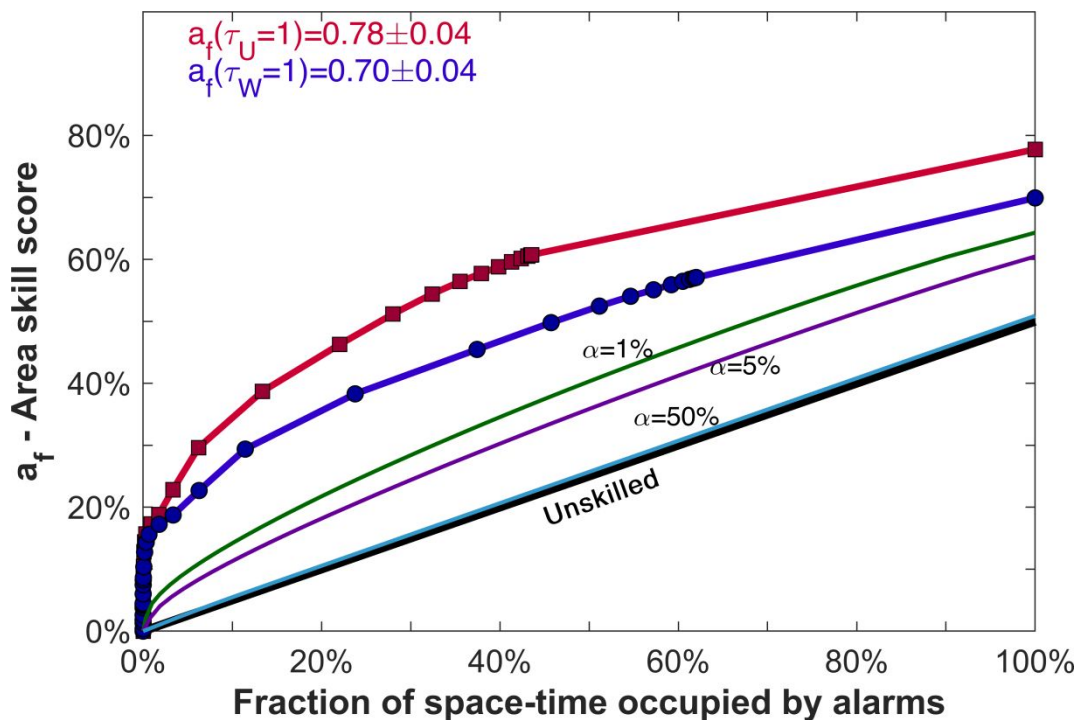
Figure S6 – Same as Fig. S3 for declustered (first) target shocks with Mw≥5.0 (see text).
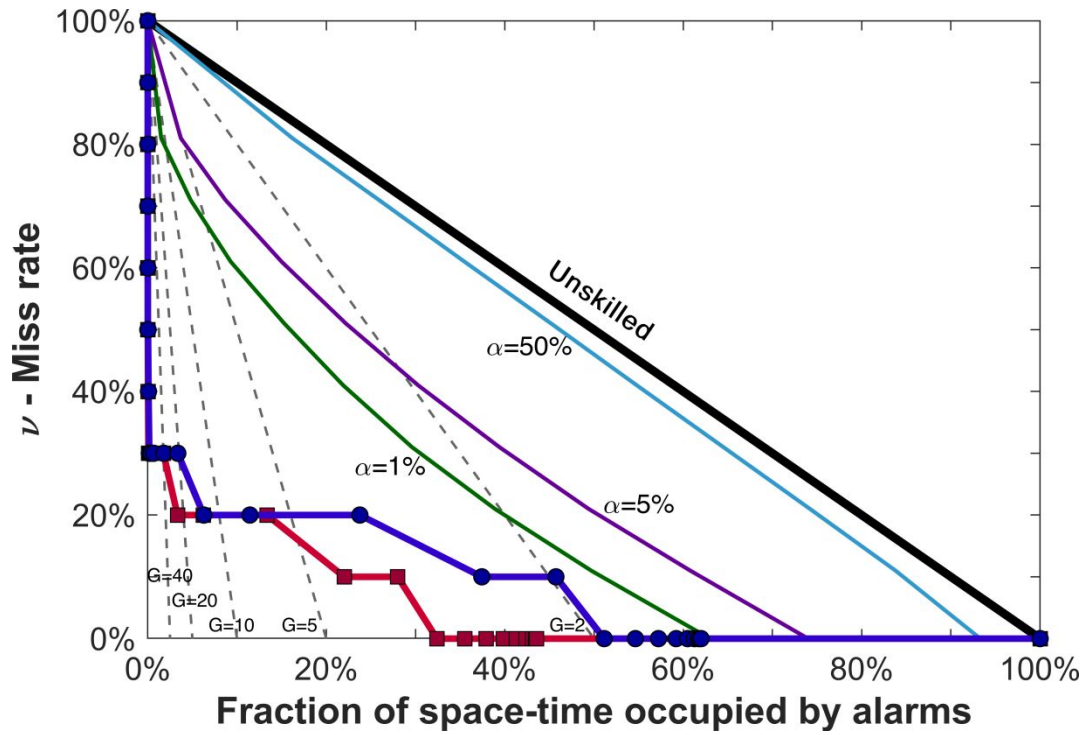
Figure S7 – Same as Fig. S2 for all target shocks with Mw≥6.0 (not-declustered).
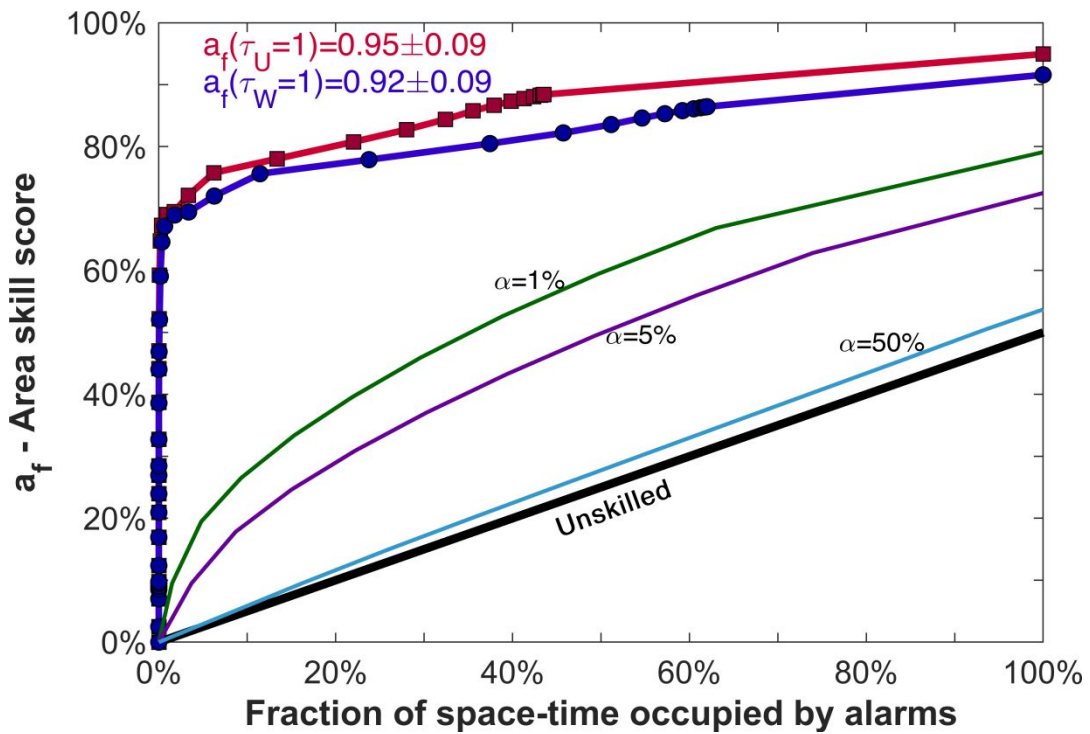
Figure S8 – Same as Fig. S3 for all target shocks with Mw≥6.0 (not-declustered).
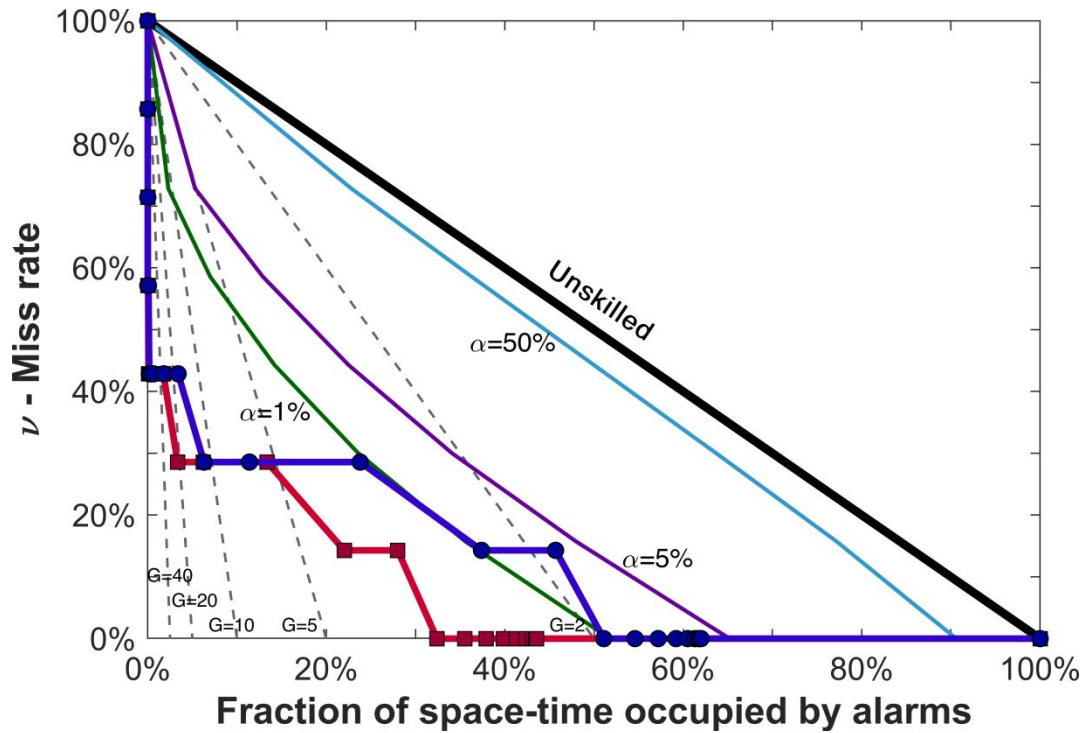
Figure S9 – Same as Fig. S2 for declustered (first) target shocks with Mw≥6.0.
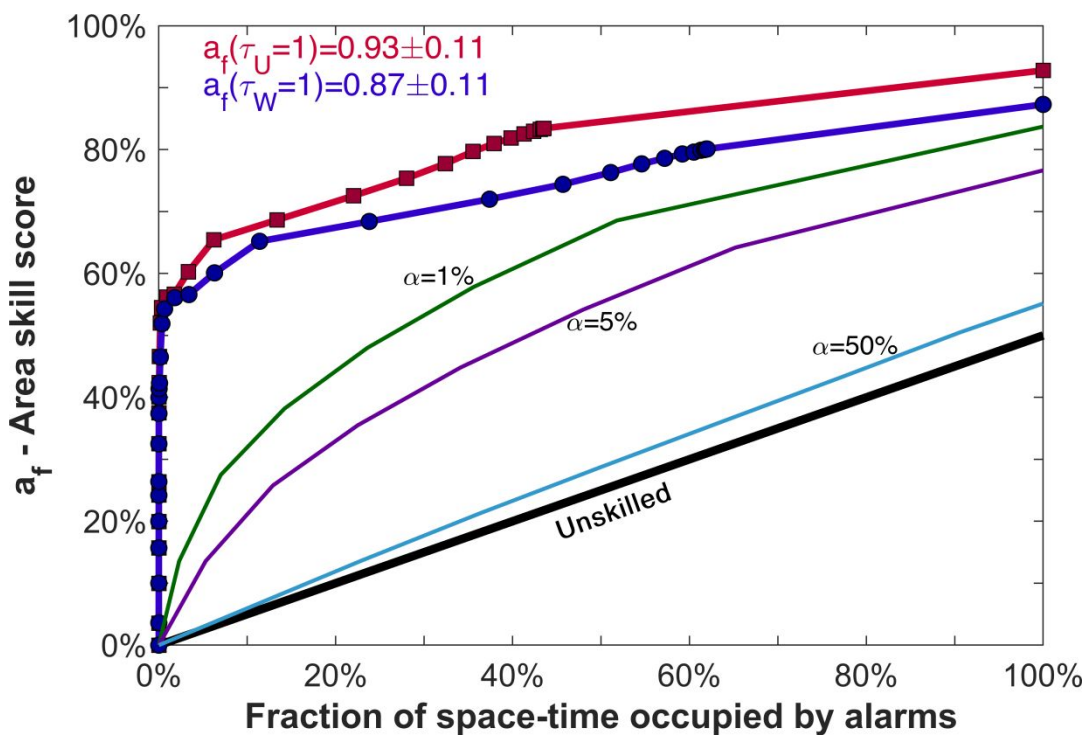
Figure S10 – Same as Fig. S3 for declustered (first) target shocks with Mw≥6.0.
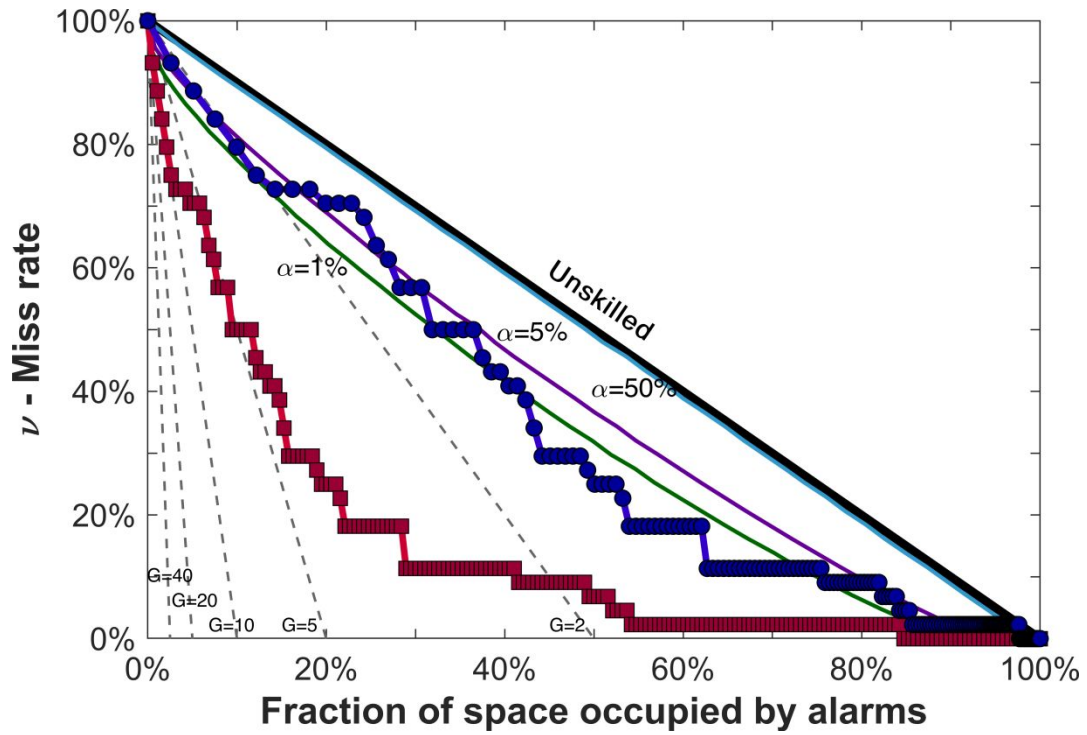
Figure S11 – Same as Fig. S2 for time-independent analysis of declustered (first) target shocks with Mw≥5.0.
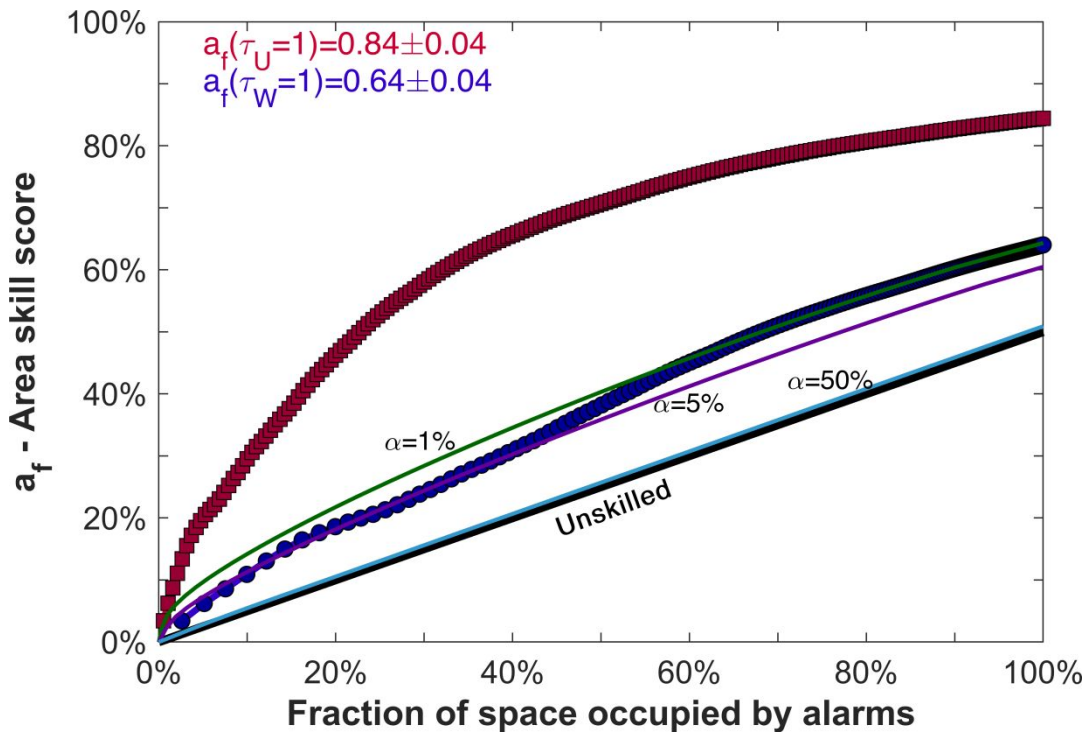
Figure S12 – Same as Fig. S3 for time-independent analysis of declustered (first) target shocks with Mw≥5.0.
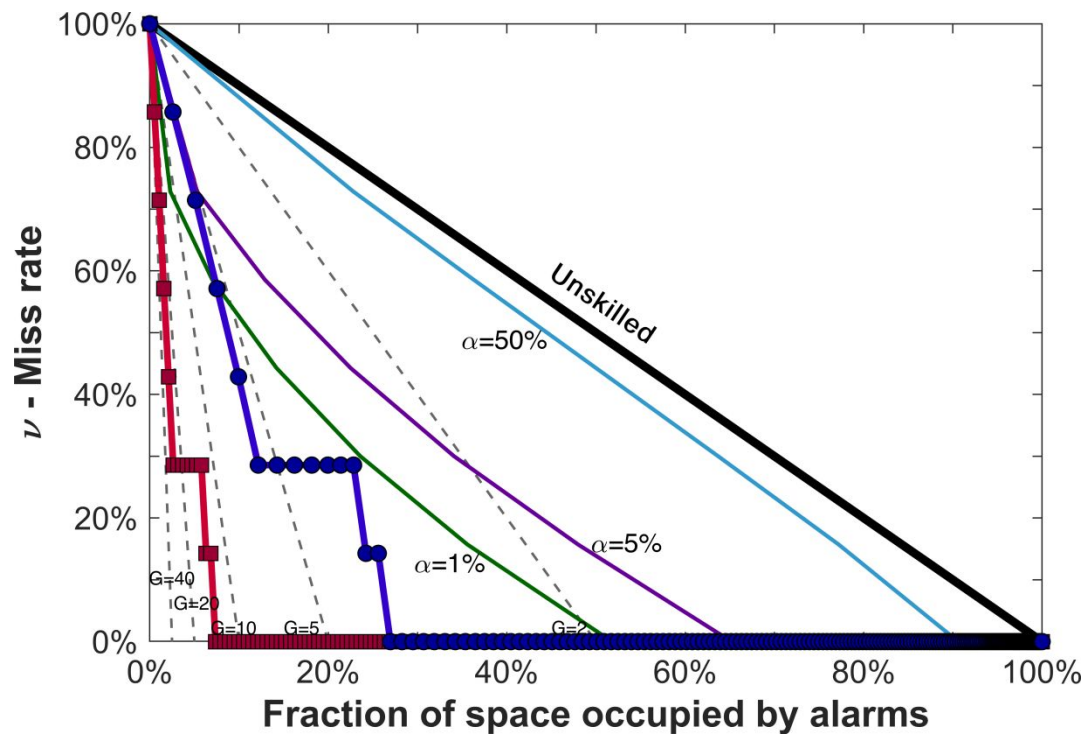
Figure S13 – Same as Fig. S2 for time-independent analysis of declustered (first) target shocks with
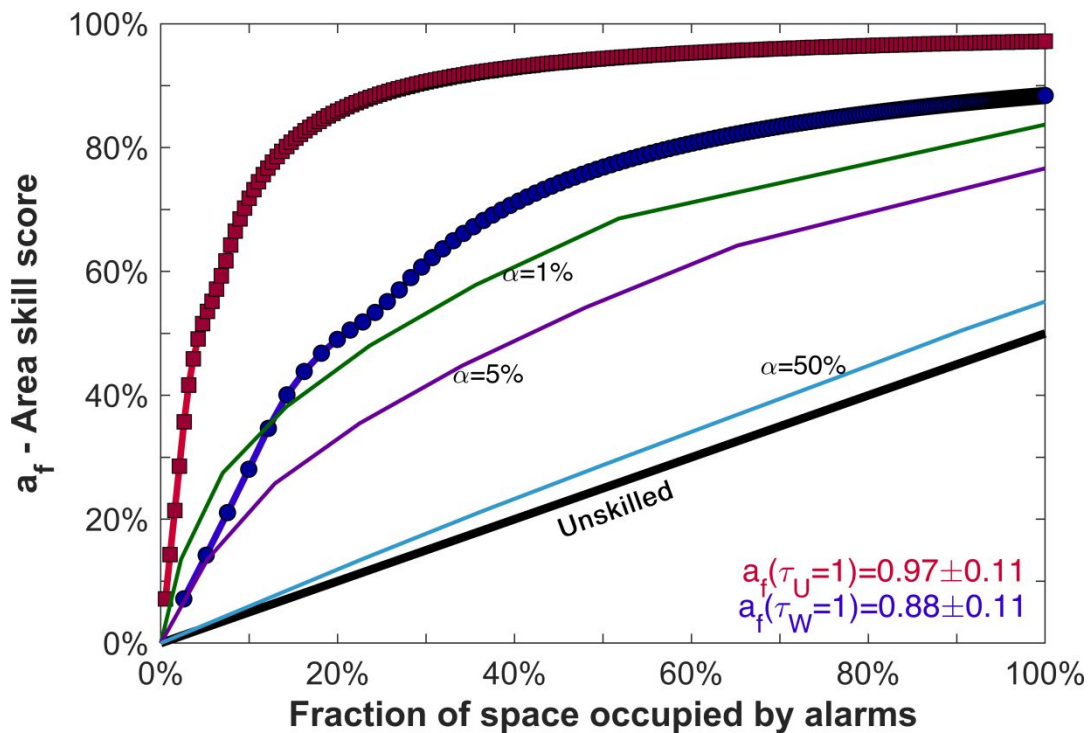
Mw≥6.0.

Figure S14 – Same as Fig. S3 for time-independent analysis of declustered (first) target shocks with

Mw≥6.0.
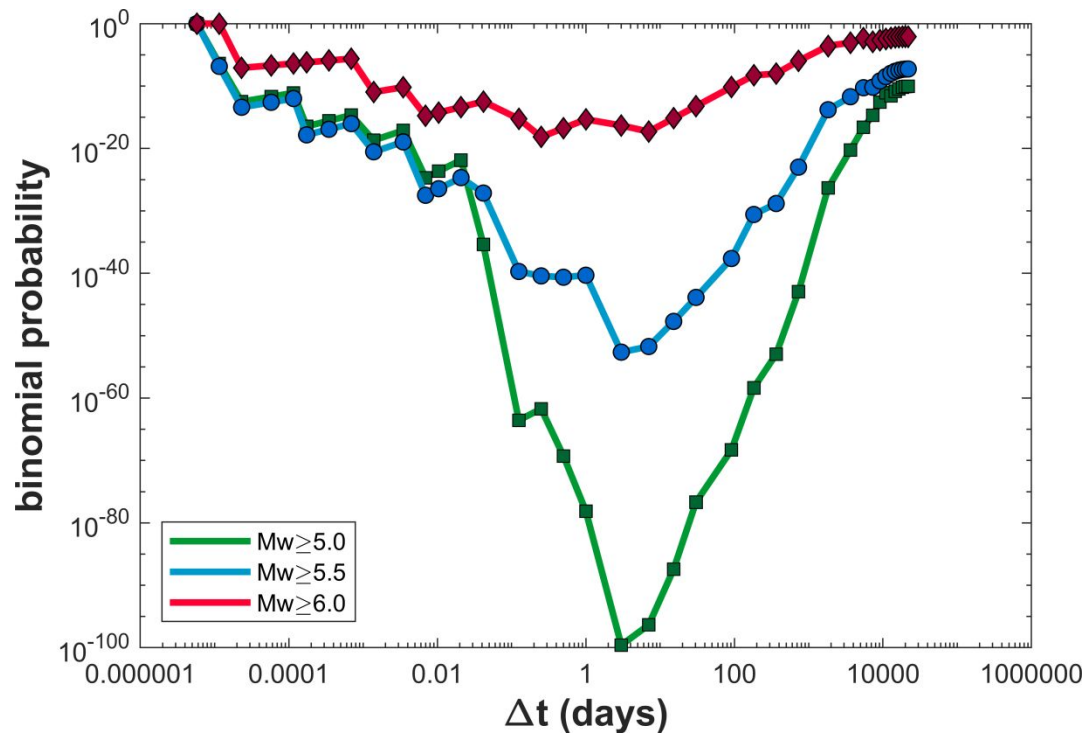
Figure S15 – Binomial probability density for all target shocks (not-declustered) and weighted fraction of space-time occupied by alarms for different magnitude thresholds (see inset) as a function of the alarm duration Δt.
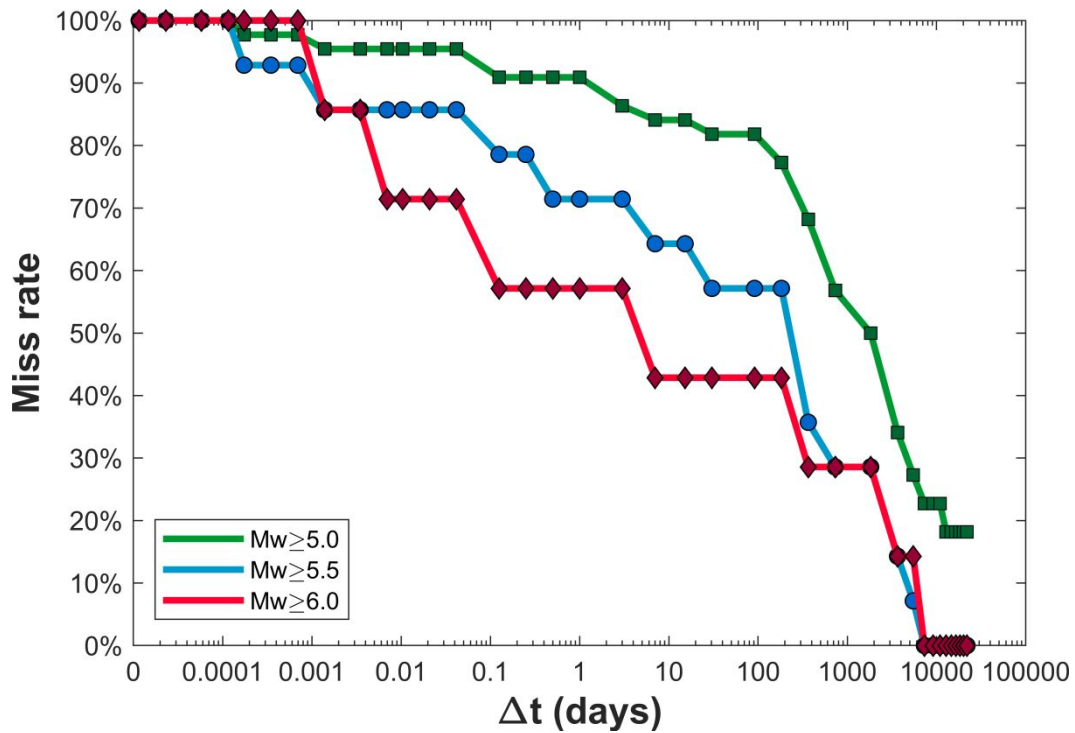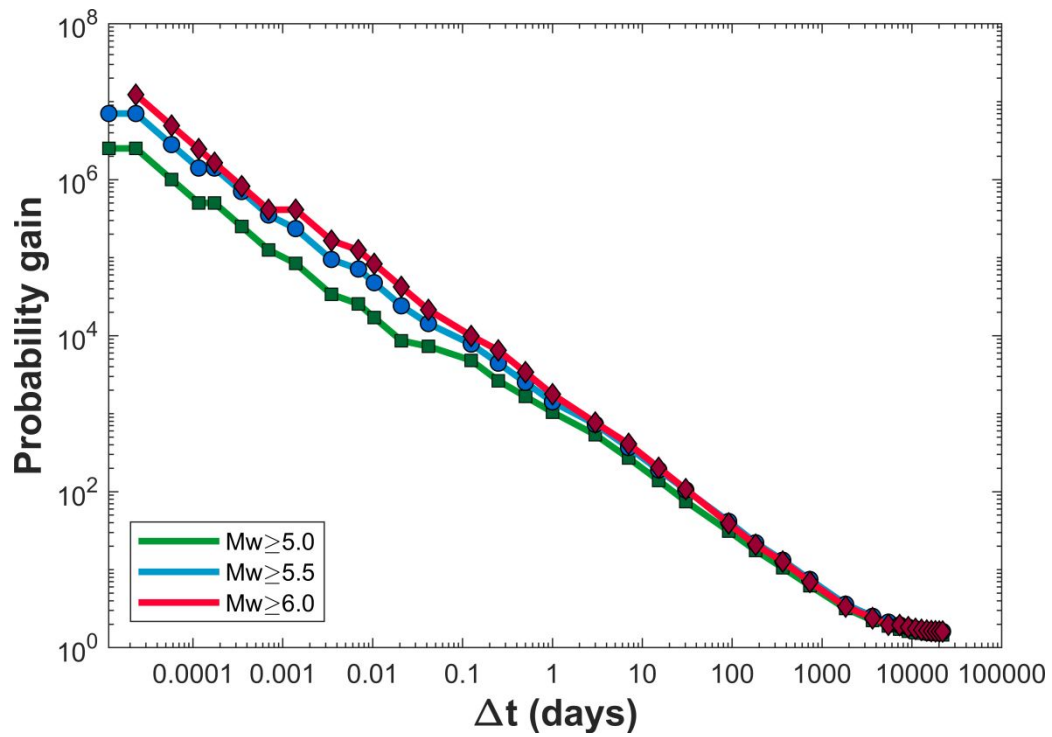
Figure S16 – Probability gain for all target shocks (not-declustered) and weighted fraction of space-time occupied by alarms for different magnitude thresholds (see inset) as a function of the alarm duration Δt.

1
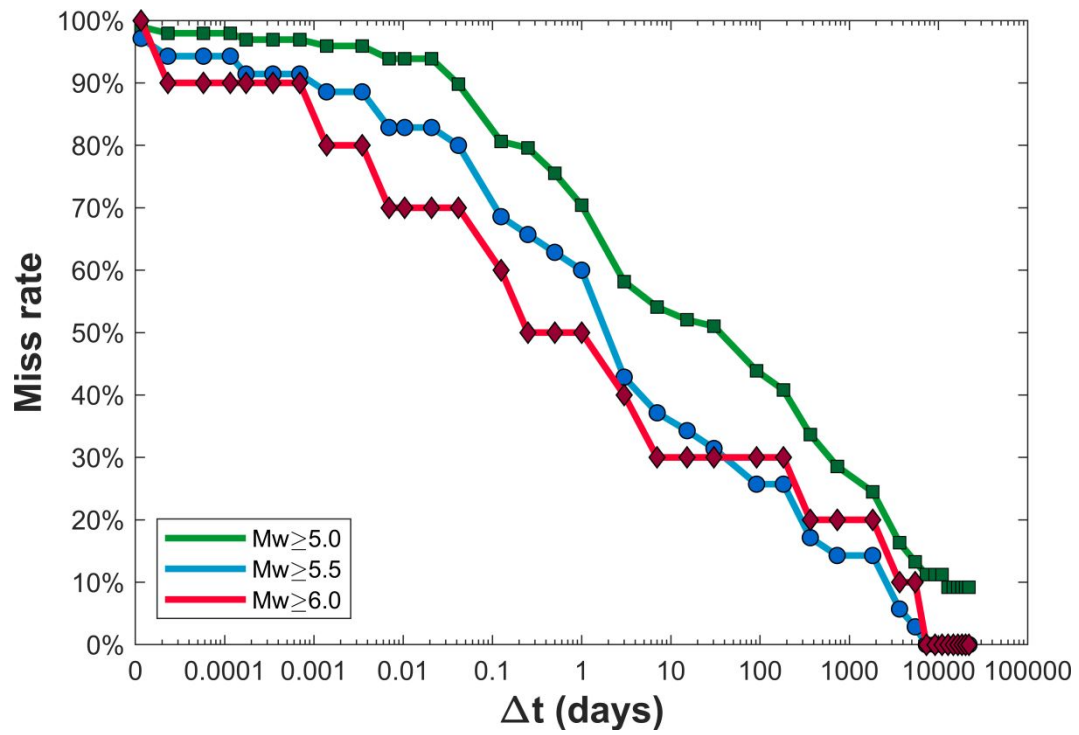
Figure S17 – Miss rate for all target shocks (not-declustered) for different magnitude thresholds (see inset) as a function of the alarm duration Δt.

1

Table S1 – List of center coordinates of circular areas (CA) with radius of 30 km.

Nc	Latitude	Longitude	$N_{4.5}$	$N_{5.0}$	$N_{5.5}$	$N_{6.0}$	$\lambda_{4.5}$	$\lambda_{5.0}$	$\lambda_{5.5}$	$\lambda_{6.0}$	λ_{ave}	w
1	47.0000	11.4757	4	2	0	0	0.1581	0.2500	-	-	0.2041	0.004107
2	47.0000	12.0351	1	1	0	0	0.0395	0.1250	-	-	0.0823	0.001656
3	46.6185	10.3330	4	0	0	0	0.1581	-	-	-	0.1581	0.003182
4	46.6185	10.8885	2	0	0	0	0.0791	-	-	-	0.0791	0.001591
5	46.6185	11.4440	2	0	0	0	0.0791	-	-	-	0.0791	0.001591
6	46.6185	11.9995	1	0	0	0	0.0395	-	-	-	0.0395	0.000796
7	46.6185	12.5550	5	1	0	0	0.1976	0.1250	-	-	0.1613	0.003247
8	46.6185	13.1105	15	8	2	1	0.5929	1.0000	0.3514	0.2941	0.5596	0.011263
9	46.2369	9.7581	1	0	0	0	0.0395	-	-	-	0.0395	0.000796
10	46.2369	10.3098	1	0	0	0	0.0395	-	-	-	0.0395	0.000796
11	46.2369	10.8614	1	0	0	0	0.0395	-	-	-	0.0395	0.000796
12	46.2369	11.9647	1	1	0	0	0.0395	0.1250	-	-	0.0823	0.001656
13	46.2369	12.5163	9	1	4	2	0.3558	0.1250	0.7027	0.5882	0.4429	0.008915
14	46.2369	13.0679	34	16	7	2	1.3440	2.0000	1.2298	0.5882	1.2905	0.025974
15	46.2369	13.6195	11	5	2	0	0.4348	0.6250	0.3514	-	0.4704	0.009468
16	45.8554	8.0957	0	0	0	0	-	-	-	-	0.0395	0.000796
17	45.8554	9.1913	1	0	0	0	0.0395	-	-	-	0.0395	0.000796
18	45.8554	9.7392	4	0	0	0	0.1581	-	-	-	0.1581	0.003182
19	45.8554	10.2870	5	0	0	0	0.1976	-	-	-	0.1976	0.003978
20	45.8554	10.8348	8	2	0	0	0.3162	0.2500	-	-	0.2831	0.005698
21	45.8554	11.3827	2	0	0	0	0.0791	-	-	-	0.0791	0.001591
22	45.8554	11.9305	6	3	1	1	0.2372	0.3750	0.1757	0.2941	0.2705	0.005444
23	45.8554	12.4783	6	1	2	1	0.2372	0.1250	0.3514	0.2941	0.2519	0.005070
24	45.8554	13.0262	0	0	0	0	-	-	-	-	0.0395	0.000796
25	45.8554	13.5740	1	1	0	0	0.0395	0.1250	-	-	0.0823	0.001656
26	45.4738	7.0000	0	0	0	0	-	-	-	-	0.0395	0.000796
27	45.4738	7.5441	3	0	0	0	0.1186	-	-	-	0.1186	0.002387
28	45.4738	8.0882	3	0	0	0	0.1186	-	-	-	0.1186	0.002387
29	45.4738	8.6323	1	0	0	0	0.0395	-	-	-	0.0395	0.000796
30	45.4738	9.1764	1	0	0	0	0.0395	-	-	-	0.0395	0.000796
31	45.4738	9.7206	3	1	1	0	0.1186	0.1250	0.1757	-	0.1398	0.002813
32	45.4738	10.2647	6	1	0	0	0.2372	0.1250	-	-	0.1811	0.003645
33	45.4738	10.8088	9	4	1	0	0.3558	0.5000	0.1757	-	0.3438	0.006920
34	45.4738	11.3529	5	1	1	0	0.1976	0.1250	0.1757	-	0.1661	0.003343
35	45.4738	11.8970	0	0	0	0	-	-	-	-	0.0395	0.000796
36	45.4738	12.4411	0	0	0	0	-	-	-	-	0.0395	0.000796
37	45.0923	7.0000	4	2	0	0	0.1581	0.2500	-	-	0.2041	0.004107
38	45.0923	7.5405	7	2	0	0	0.2767	0.2500	-	-	0.2633	0.005300
39	45.0923	8.6214	3	0	0	0	0.1186	-	-	-	0.1186	0.002387
40	45.0923	9.1619	2	1	0	0	0.0791	0.1250	-	-	0.1020	0.002054
41	45.0923	9.7023	1	1	0	0	0.0395	0.1250	-	-	0.0823	0.001656
42	45.0923	10.2428	1	1	0	0	0.0395	0.1250	-	-	0.0823	0.001656
43	45.0923	10.7832	6	1	1	0	0.2372	0.1250	0.1757	-	0.1793	0.003608
44	45.0923	11.3237	8	3	1	1	0.3162	0.3750	0.1757	0.2941	0.2903	0.005842

1

45	45.0923	11.8642	0	0	0	0	-	-	-	-	0.0395	0.000796
46	44.7107	7.0000	3	1	1	0	0.1186	0.1250	0.1757	-	0.1398	0.002813
47	44.7107	7.5369	2	0	1	0	0.0791	-	0.1757	-	0.1274	0.002564
48	44.7107	8.0738	0	0	0	0	-	-	-	-	0.0395	0.000796
49	44.7107	8.6107	4	0	0	0	0.1581	-	-	-	0.1581	0.003182
50	44.7107	9.1476	7	1	1	0	0.2767	0.1250	0.1757	-	0.1925	0.003874
51	44.7107	9.6844	6	0	0	0	0.2372	-	-	-	0.2372	0.004774
52	44.7107	10.2213	11	5	2	0	0.4348	0.6250	0.3514	-	0.4704	0.009468
53	44.7107	10.7582	19	4	3	0	0.7510	0.5000	0.5270	-	0.5927	0.011929
54	44.7107	11.2951	20	10	2	1	0.7906	1.2500	0.3514	0.2941	0.6715	0.013515
55	44.7107	11.8320	7	2	0	0	0.2767	0.2500	-	-	0.2633	0.005300
56	44.7107	12.3689	2	0	0	0	0.0791	-	-	-	0.0791	0.001591
57	44.3292	7.0000	5	1	0	0	0.1976	0.1250	-	-	0.1613	0.003247
58	44.3292	7.5334	5	0	0	0	0.1976	-	-	-	0.1976	0.003978
59	44.3292	8.0668	3	0	0	0	0.1186	-	-	-	0.1186	0.002387
60	44.3292	8.6002	0	0	0	0	-	-	-	-	0.0395	0.000796
61	44.3292	9.1335	0	0	0	0	-	-	-	-	0.0395	0.000796
62	44.3292	9.6669	5	2	1	0	0.1976	0.2500	0.1757	-	0.2078	0.004182
63	44.3292	10.2003	19	8	4	1	0.7510	1.0000	0.7027	0.2941	0.6870	0.013827
64	44.3292	10.7337	9	2	0	0	0.3558	0.2500	-	-	0.3029	0.006096
65	44.3292	11.2671	20	8	0	0	0.7906	1.0000	-	-	0.8953	0.018019
66	44.3292	11.8005	15	3	2	1	0.5929	0.3750	0.3514	0.2941	0.4034	0.008118
67	44.3292	12.3338	6	2	2	0	0.2372	0.2500	0.3514	-	0.2795	0.005626
68	43.9476	7.5299	0	0	1	0	-	-	0.1757	-	0.1757	0.003536
69	43.9476	8.0599	4	1	2	1	0.1581	0.1250	0.3514	0.2941	0.2321	0.004672
70	43.9476	9.6497	0	0	0	0	-	-	-	-	0.0395	0.000796
71	43.9476	10.1797	13	2	2	1	0.5139	0.2500	0.3514	0.2941	0.3523	0.007091
72	43.9476	10.7096	12	2	1	0	0.4743	0.2500	0.1757	-	0.3000	0.006038
73	43.9476	11.2396	14	4	2	1	0.5534	0.5000	0.3514	0.2941	0.4247	0.008548
74	43.9476	11.7695	25	4	2	2	0.9882	0.5000	0.3514	0.5882	0.6070	0.012216
75	43.9476	12.2995	11	4	3	0	0.4348	0.5000	0.5270	-	0.4873	0.009808
76	43.9476	12.8294	22	12	3	0	0.8696	1.5000	0.5270	-	0.9656	0.019434
77	43.9476	13.3594	5	3	1	0	0.1976	0.3750	0.1757	-	0.2494	0.005020
78	43.5661	10.1595	2	0	0	0	0.0791	-	-	-	0.0791	0.001591
79	43.5661	10.6861	4	0	1	1	0.1581	-	0.1757	0.2941	0.2093	0.004213
80	43.5661	11.2126	9	2	1	0	0.3558	0.2500	0.1757	-	0.2605	0.005243
81	43.5661	11.7392	2	0	0	0	0.0791	-	-	-	0.0791	0.001591
82	43.5661	12.2658	8	4	3	1	0.3162	0.5000	0.5270	0.2941	0.4093	0.008239
83	43.5661	12.7924	3	1	1	2	0.1186	0.1250	0.1757	0.5882	0.2519	0.005069
84	43.5661	13.3190	7	3	1	1	0.2767	0.3750	0.1757	0.2941	0.2804	0.005643
85	43.5661	13.8455	3	2	0	0	0.1186	0.2500	-	-	0.1843	0.003709
86	43.1845	10.6629	3	0	0	0	0.1186	-	-	-	0.1186	0.002387
87	43.1845	11.1862	3	2	0	0	0.1186	0.2500	-	-	0.1843	0.003709
88	43.1845	11.7095	1	1	0	0	0.0395	0.1250	-	-	0.0823	0.001656
89	43.1845	12.2328	9	2	2	0	0.3558	0.2500	0.3514	-	0.3190	0.006421
90	43.1845	12.7561	25	10	6	3	0.9882	1.2500	1.0541	0.8824	1.0437	0.021006
91	43.1845	13.2793	9	2	2	1	0.3558	0.2500	0.3514	0.2941	0.3128	0.006296

1

92	43.1845	13.8026	4	2	0	0	0.1581	0.2500	-	-	0.2041	0.004107
93	42.8030	11.1603	0	0	0	0	-	-	-	-	0.0395	0.000796
94	42.8030	11.6803	10	2	0	0	0.3953	0.2500	-	-	0.3226	0.006494
95	42.8030	12.2004	6	1	0	0	0.2372	0.1250	-	-	0.1811	0.003645
96	42.8030	12.7204	37	13	8	1	1.4626	1.6250	1.4055	0.2941	1.1968	0.024088
97	42.8030	13.2405	34	12	6	3	1.3440	1.5000	1.0541	0.8824	1.1951	0.024054
98	42.8030	13.7605	3	2	1	0	0.1186	0.2500	0.1757	-	0.1814	0.003651
99	42.4214	11.6518	3	0	0	0	0.1186	-	-	-	0.1186	0.002387
100	42.4214	12.1686	1	0	0	0	0.0395	-	-	-	0.0395	0.000796
101	42.4214	12.6855	12	3	2	0	0.4743	0.3750	0.3514	-	0.4002	0.008056
102	42.4214	13.2024	29	17	5	3	1.1463	2.1250	0.8784	0.8824	1.2580	0.025320
103	42.4214	13.7192	11	8	3	1	0.4348	1.0000	0.5270	0.2941	0.5640	0.011351
104	42.4214	14.2361	2	2	0	0	0.0791	0.2500	-	-	0.1645	0.003311
105	42.0399	11.6237	0	0	0	0	-	-	-	-	0.0395	0.000796
106	42.0399	12.1375	1	0	0	0	0.0395	-	-	-	0.0395	0.000796
107	42.0399	12.6512	6	3	0	0	0.2372	0.3750	-	-	0.3061	0.006161
108	42.0399	13.1650	12	1	1	0	0.4743	0.1250	0.1757	-	0.2583	0.005200
109	42.0399	13.6787	15	5	1	1	0.5929	0.6250	0.1757	0.2941	0.4219	0.008492
110	42.0399	14.1925	5	4	1	1	0.1976	0.5000	0.1757	0.2941	0.2919	0.005874
111	42.0399	14.7062	0	0	0	0	-	-	-	-	0.0395	0.000796
112	42.0399	15.2200	4	0	1	0	0.1581	-	0.1757	-	0.1669	0.003359
113	42.0399	15.7337	4	2	0	1	0.1581	0.2500	-	0.2941	0.2341	0.004711
114	42.0399	16.2475	1	0	0	1	0.0395	-	-	0.2941	0.1668	0.003358
115	41.6583	12.1069	1	0	0	0	0.0395	-	-	-	0.0395	0.000796
116	41.6583	12.6176	10	4	1	0	0.3953	0.5000	0.1757	-	0.3570	0.007185
117	41.6583	13.1283	3	0	0	0	0.1186	-	-	-	0.1186	0.002387
118	41.6583	13.6390	19	4	0	1	0.7510	0.5000	-	0.2941	0.5151	0.010366
119	41.6583	14.1497	12	4	1	0	0.4743	0.5000	0.1757	-	0.3833	0.007715
120	41.6583	14.6604	7	3	3	1	0.2767	0.3750	0.5270	0.2941	0.3682	0.007411
121	41.6583	15.1711	7	2	2	2	0.2767	0.2500	0.3514	0.5882	0.3666	0.007378
122	41.6583	15.6818	18	10	2	1	0.7115	1.2500	0.3514	0.2941	0.6517	0.013118
123	41.6583	16.1925	11	6	0	0	0.4348	0.7500	-	-	0.5924	0.011923
124	41.2768	9.0308	1	0	0	0	0.0395	-	-	-	0.0395	0.000796
125	41.2768	16.1385	1	0	0	0	0.0395	-	-	-	0.0395	0.000796
126	41.2768	13.0924	0	0	0	0	-	-	-	-	0.0395	0.000796
127	41.2768	13.6001	0	0	0	0	-	-	-	-	0.0395	0.000796
128	41.2768	14.1077	6	1	0	0	0.2372	0.1250	-	-	0.1811	0.003645
129	41.2768	14.6154	8	3	2	3	0.3162	0.3750	0.3514	0.8824	0.4812	0.009686
130	41.2768	15.1231	11	5	3	4	0.4348	0.6250	0.5270	1.1765	0.6908	0.013904
131	41.2768	15.6308	3	0	0	1	0.1186	-	-	0.2941	0.2064	0.004153
132	41.2768	16.6462	0	0	0	0	-	-	-	-	0.0395	0.000796
133	40.8952	9.0190	1	0	0	0	0.0395	-	-	-	0.0395	0.000796
134	40.8952	14.0666	0	0	0	0	-	-	-	-	0.0395	0.000796
135	40.8952	14.5714	6	0	0	0	0.2372	-	-	-	0.2372	0.004774
136	40.8952	15.0761	21	7	4	5	0.8301	0.8750	0.7027	1.4706	0.9696	0.019515
137	40.8952	15.5809	31	9	5	4	1.2254	1.1250	0.8784	1.1765	1.1013	0.022166
138	40.8952	16.0856	2	1	0	0	0.0791	0.1250	-	-	0.1020	0.002054

1

139	40.8952	16.5904	1	0	0	0	0.0395	-	-	-	0.0395	0.000796
140	40.5137	14.5281	0	0	0	0	-	-	-	-	0.0395	0.000796
141	40.5137	15.0300	1	1	0	0	0.0395	0.1250	-	-	0.0823	0.001656
142	40.5137	15.5318	20	3	1	0	0.7906	0.3750	0.1757	-	0.4471	0.008998
143	40.5137	16.0337	9	2	2	1	0.3558	0.2500	0.3514	0.2941	0.3128	0.006296
144	40.5137	16.5356	4	1	0	0	0.1581	0.1250	-	-	0.1416	0.002849
145	40.5137	17.0375	1	0	0	0	0.0395	-	-	-	0.0395	0.000796
146	40.5137	17.5393	0	0	0	0	-	-	-	-	0.0395	0.000796
147	40.1321	15.4838	2	0	2	0	0.0791	-	0.3514	-	0.2152	0.004332
148	40.1321	15.9828	9	4	4	1	0.3558	0.5000	0.7027	0.2941	0.4632	0.009322
149	40.1321	16.4819	1	0	0	0	0.0395	-	-	-	0.0395	0.000796
150	40.1321	17.9790	1	0	0	0	0.0395	-	-	-	0.0395	0.000796
151	39.7506	15.9329	4	3	0	0	0.1581	0.3750	-	-	0.2666	0.005365
152	39.7506	16.4291	6	3	2	0	0.2372	0.3750	0.3514	-	0.3212	0.006464
153	39.7506	16.9254	5	1	1	1	0.1976	0.1250	0.1757	0.2941	0.1981	0.003987
154	39.3690	8.9742	0	0	0	0	-	-	-	-	0.0395	0.000796
155	39.3690	15.8838	1	1	1	0	0.0395	0.1250	0.1757	-	0.1134	0.002282
156	39.3690	16.3774	9	3	6	2	0.3558	0.3750	1.0541	0.5882	0.5933	0.011941
157	39.3690	16.8709	1	0	1	2	0.0395	-	0.1757	0.5882	0.2678	0.005390
158	38.9875	8.9635	0	0	0	0	-	-	-	-	0.0395	0.000796
159	38.9875	15.3449	6	3	0	0	0.2372	0.3750	-	-	0.3061	0.006161
160	38.9875	15.8358	1	1	1	1	0.0395	0.1250	0.1757	0.2941	0.1586	0.003192
161	38.9875	16.3266	4	0	3	5	0.1581	-	0.5270	1.4706	0.7186	0.014463
162	38.9875	16.8175	3	0	1	1	0.1186	-	0.1757	0.2941	0.1961	0.003947
163	38.6059	14.8121	8	3	0	0	0.3162	0.3750	-	-	0.3456	0.006956
164	38.6059	15.3003	7	3	0	0	0.2767	0.3750	-	-	0.3258	0.006558
165	38.6059	15.7886	5	2	2	1	0.1976	0.2500	0.3514	0.2941	0.2733	0.005500
166	38.6059	16.2768	7	1	4	4	0.2767	0.1250	0.7027	1.1765	0.5702	0.011477
167	38.6059	16.7651	1	1	1	0	0.0395	0.1250	0.1757	-	0.1134	0.002282
168	38.2244	13.3139	4	1	0	0	0.1581	0.1250	-	-	0.1416	0.002849
169	38.2244	13.7996	7	3	1	0	0.2767	0.3750	0.1757	-	0.2758	0.005551
170	38.2244	14.7709	6	1	1	1	0.2372	0.1250	0.1757	0.2941	0.2080	0.004186
171	38.2244	15.2566	13	2	2	2	0.5139	0.2500	0.3514	0.5882	0.4259	0.008571
172	38.2244	15.7423	13	6	4	3	0.5139	0.7500	0.7027	0.8824	0.7122	0.014335
173	38.2244	16.2280	3	2	2	1	0.1186	0.2500	0.3514	0.2941	0.2535	0.005103
174	37.8428	12.7979	15	6	2	1	0.5929	0.7500	0.3514	0.2941	0.4971	0.010005
175	37.8428	13.2811	9	6	1	1	0.3558	0.7500	0.1757	0.2941	0.3939	0.007928
176	37.8428	13.7642	2	1	0	0	0.0791	0.1250	-	-	0.1020	0.002054
177	37.8428	14.2474	11	3	0	0	0.4348	0.3750	-	-	0.4049	0.008150
178	37.8428	14.7306	8	2	0	0	0.3162	0.2500	-	-	0.2831	0.005698
179	37.8428	15.2137	12	2	2	1	0.4743	0.2500	0.3514	0.2941	0.3425	0.006893
180	37.8428	15.6969	0	0	0	0	-	-	-	-	0.0395	0.000796
181	37.8428	16.1800	3	1	0	0	0.1186	0.1250	-	-	0.1218	0.002451
182	37.4613	12.7682	4	0	0	0	0.1581	-	-	-	0.1581	0.003182
183	37.4613	13.2489	1	0	0	0	0.0395	-	-	-	0.0395	0.000796
184	37.4613	13.7296	0	0	0	0	-	-	-	-	0.0395	0.000796
185	37.4613	14.6909	6	2	1	0	0.2372	0.2500	0.1757	-	0.2210	0.004447

1

186	37.4613	15.1716	8	3	3	1	0.3162	0.3750	0.5270	0.2941	0.3781	0.007610
187	37.0797	14.6521	5	2	1	0	0.1976	0.2500	0.1757	-	0.2078	0.004182
188	37.0797	15.1303	1	0	0	2	0.0395	-	-	0.5882	0.3139	0.006317
189	36.6982	14.6139	1	1	0	0	0.0395	0.1250	-	-	0.0823	0.001656
190	36.6982	15.0898	0	0	0	0	-	-	-	-	0.0395	0.000796

$N_{4.5}$, $N_{5.0}$, $N_{5.5}$, $N_{6.0}$: numbers of earthquakes occurred within each CA, according to the CPTI15 catalogue up to year 1959, with Mw≥4.5, 5.0, 5.5 and 6.0 respectively in respective time intervals of completeness. $\lambda_{4.5}$, $\lambda_{5.0}$, $\lambda_{5.5}$, $\lambda_{6.0}$: average rates (events/y) of earthquakes with Mw≥4.0 within each CA computed from observed earthquakes with Mw≥4.5, 5.0, 5.5 and 6.0 respectively and assuming a b-value=1 (see text). λ_{ave}: average of non-null rates $\lambda_{4.5}$, $\lambda_{5.0}$, $\lambda_{5.5}$, $\lambda_{6.0}$. $w = \lambda_{ave}/\Sigma\lambda_{ave}$: overall weight of each CA ($\Sigma w = 1$).

1

Table S2 – Values of variables in Molchan and Area Skill score plots of Fig. 2 and 3 for Mw≥5.5 not-declustered targets.

Δt (years)	Δt (days)	τ_u	τ_w	h	ν	$a_f(\tau_u)$	$a_f(\tau_w)$
1.6E-08	5.8E-06	8.6E-10	2.0E-09	0	1.000	0.000	0.000
3.2E-08	1.2E-05	1.7E-09	4.1E-09	1	0.971	0.021	0.022
6.3E-08	2.3E-05	3.4E-09	8.1E-09	2	0.943	0.037	0.038
1.6E-07	5.8E-05	8.6E-09	2.0E-08	2	0.943	0.051	0.051
3.2E-07	1.2E-04	1.7E-08	4.1E-08	2	0.943	0.054	0.054
4.8E-07	1.7E-04	2.6E-08	6.1E-08	3	0.914	0.060	0.060
9.5E-07	3.5E-04	5.1E-08	1.2E-07	3	0.914	0.073	0.073
1.9E-06	6.9E-04	1.0E-07	2.4E-07	3	0.914	0.080	0.080
3.8E-06	1.4E-03	2.0E-07	4.9E-07	4	0.886	0.090	0.090
9.5E-06	3.5E-03	5.1E-07	1.2E-06	4	0.886	0.104	0.104
1.9E-05	6.9E-03	1.0E-06	2.4E-06	6	0.829	0.124	0.124
2.9E-05	1.0E-02	1.5E-06	3.6E-06	6	0.829	0.140	0.139
5.7E-05	2.1E-02	3.0E-06	7.1E-06	6	0.829	0.155	0.155
1.1E-04	4.2E-02	6.0E-06	1.4E-05	7	0.800	0.170	0.170
3.4E-04	0.13	1.7E-05	4.0E-05	11	0.686	0.227	0.227
6.8E-04	0.25	3.4E-05	7.7E-05	12	0.657	0.276	0.276
1.4E-03	0.50	6.5E-05	1.5E-04	13	0.629	0.316	0.314
2.7E-03	1.00	1.3E-04	2.8E-04	14	0.600	0.350	0.349
8.2E-03	3.00	3.6E-04	7.8E-04	20	0.429	0.438	0.436
0.019	7.02	8.1E-04	1.7E-03	22	0.371	0.527	0.525
0.042	15.22	1.7E-03	3.5E-03	23	0.343	0.587	0.585
0.083	30.44	3.2E-03	6.5E-03	24	0.314	0.628	0.625
0.250	91.31	9.1E-03	0.018	26	0.257	0.684	0.682
0.500	182.62	0.017	0.034	26	0.257	0.712	0.710
1.000	365.24	0.033	0.063	29	0.171	0.747	0.745
2.000	730.49	0.062	0.114	30	0.143	0.791	0.789
5.000	1826.21	0.134	0.238	30	0.143	0.827	0.825
10	3652.43	0.220	0.374	33	0.057	0.855	0.852
15	5478.64	0.280	0.457	34	0.029	0.877	0.871
20	7304.85	0.324	0.511	35	0.000	0.892	0.883
25	9131.06	0.355	0.546	35	0.000	0.901	0.891
30	10957.28	0.379	0.572	35	0.000	0.908	0.896
35	12783.49	0.398	0.592	35	0.000	0.912	0.899
40	14609.70	0.413	0.605	35	0.000	0.915	0.901
45	16435.91	0.424	0.613	35	0.000	0.917	0.903
50	18262.13	0.431	0.617	35	0.000	0.919	0.903
55	20088.34	0.434	0.619	35	0.000	0.919	0.904
60	21914.55	0.436	0.620	35	0.000	0.920	0.904
Full occ.	Full occ.	1.000	1.000	35	0.000	0.965	0.940

Δt is the duration of alarms, τ_u and τ_w the unweighted and weighted fraction of space-time occupied by alarms respectively, h the number of successful forecasts, ν the miss rate, $a_f(\tau_u)$ and $a_f(\tau_w)$ the Area Skill scores computed considering the unweighted and weighted fraction of space-time occupied

by alarms respectively. The last row (Δt= Full occ.) reports values for a full occupation of the space-time by alarms.

Table S3 – Same as Table S2 for Mw≥5.5 declustered targets (Fig. 4 and 5).

Δt (years)	Δt (days)	τ_u	τ_w	h	ν	$a_f(\tau_u)$	$a_f(\tau_w)$
1.6E-08	5.8E-06	8.6E-10	2.0E-09	0	1.000	0.000	0.000
3.2E-08	1.2E-05	1.7E-09	4.1E-09	0	1.000	0.000	0.000
6.3E-08	2.3E-05	3.4E-09	8.1E-09	0	1.000	0.000	0.000
1.6E-07	5.8E-05	8.6E-09	2.0E-08	0	1.000	0.000	0.000
3.2E-07	1.2E-04	1.7E-08	4.1E-08	0	1.000	0.000	0.000
4.8E-07	1.7E-04	2.6E-08	6.1E-08	1	0.929	0.012	0.012
9.5E-07	3.5E-04	5.1E-08	1.2E-07	1	0.929	0.043	0.043
1.9E-06	6.9E-04	1.0E-07	2.4E-07	1	0.929	0.057	0.057
3.8E-06	1.4E-03	2.0E-07	4.9E-07	2	0.857	0.082	0.082
9.5E-06	3.5E-03	5.1E-07	1.2E-06	2	0.857	0.119	0.119
1.9E-05	6.9E-03	1.0E-06	2.4E-06	2	0.857	0.131	0.131
2.9E-05	1.0E-02	1.5E-06	3.6E-06	2	0.857	0.135	0.135
5.7E-05	2.1E-02	3.0E-06	7.1E-06	2	0.857	0.139	0.139
1.1E-04	4.2E-02	6.0E-06	1.4E-05	2	0.857	0.141	0.141
3.4E-04	0.13	1.7E-05	4.0E-05	3	0.786	0.166	0.165
6.8E-04	0.25	3.4E-05	7.7E-05	3	0.786	0.189	0.189
1.4E-03	0.50	6.5E-05	1.5E-04	4	0.714	0.219	0.218
2.7E-03	1.00	1.3E-04	2.8E-04	4	0.714	0.251	0.250
8.2E-03	3.00	3.6E-04	7.8E-04	4	0.714	0.274	0.273
0.019	7.02	8.1E-04	1.7E-03	5	0.643	0.300	0.299
0.042	15.22	1.7E-03	3.5E-03	5	0.643	0.329	0.329
0.083	30.44	3.2E-03	6.5E-03	6	0.571	0.360	0.359
0.250	91.31	9.1E-03	0.018	6	0.571	0.404	0.403
0.500	182.62	0.017	0.034	6	0.571	0.416	0.415
1.000	365.24	0.033	0.063	9	0.357	0.473	0.471
2.000	730.49	0.062	0.114	10	0.286	0.568	0.565
5.000	1826.21	0.134	0.238	10	0.286	0.646	0.642
10	3652.43	0.220	0.374	12	0.143	0.701	0.695
15	5478.64	0.280	0.457	13	0.071	0.742	0.731
20	7304.85	0.324	0.511	14	0.000	0.772	0.755
25	9131.06	0.355	0.546	14	0.000	0.792	0.771
30	10957.28	0.379	0.572	14	0.000	0.805	0.781
35	12783.49	0.398	0.592	14	0.000	0.815	0.789
40	14609.70	0.413	0.605	14	0.000	0.821	0.793
45	16435.91	0.424	0.613	14	0.000	0.826	0.796
50	18262.13	0.431	0.617	14	0.000	0.829	0.797
55	20088.34	0.434	0.619	14	0.000	0.830	0.798
60	21914.55	0.436	0.620	14	0.000	0.831	0.798
Full occ.	Full occ.	1.000	1.000	14	0.000	0.926	0.875

Table S4 – Same as Table S2 for Mw≥5.0 not-declustered targets (Fig. S1 and S2).

Δt (years)	Δt (days)	τ_u	τ_w	h	ν	$a_f(\tau_u)$	$a_f(\tau_w)$
1.6E-08	5.8E-06	8.6E-10	2.0E-09	0	1.000	0.000	0.000
3.2E-08	1.2E-05	1.7E-09	4.1E-09	1	0.990	0.003	0.003
6.3E-08	2.3E-05	3.4E-09	8.1E-09	2	0.980	0.009	0.009
1.6E-07	5.8E-05	8.6E-09	2.0E-08	2	0.980	0.016	0.016
3.2E-07	1.2E-04	1.7E-08	4.1E-08	2	0.980	0.018	0.018
4.8E-07	1.7E-04	2.6E-08	6.1E-08	3	0.969	0.021	0.021
9.5E-07	3.5E-04	5.1E-08	1.2E-07	3	0.969	0.026	0.026
1.9E-06	6.9E-04	1.0E-07	2.4E-07	3	0.969	0.028	0.028
3.8E-06	1.4E-03	2.0E-07	4.9E-07	4	0.959	0.032	0.032
9.5E-06	3.5E-03	5.1E-07	1.2E-06	4	0.959	0.037	0.037
1.9E-05	6.9E-03	1.0E-06	2.4E-06	6	0.939	0.044	0.044
2.9E-05	1.0E-02	1.5E-06	3.6E-06	6	0.939	0.050	0.050
5.7E-05	2.1E-02	3.0E-06	7.1E-06	6	0.939	0.055	0.055
1.1E-04	4.2E-02	6.0E-06	1.4E-05	10	0.898	0.068	0.068
3.4E-04	0.13	1.7E-05	4.0E-05	19	0.806	0.121	0.120
6.8E-04	0.25	3.4E-05	7.7E-05	20	0.796	0.159	0.158
1.4E-03	0.50	6.5E-05	1.5E-04	24	0.755	0.191	0.190
2.7E-03	1.00	1.3E-04	2.8E-04	29	0.704	0.229	0.228
8.2E-03	3.00	3.6E-04	7.8E-04	41	0.582	0.312	0.310
0.019	7.02	8.1E-04	1.7E-03	45	0.541	0.382	0.380
0.042	15.22	1.7E-03	3.5E-03	47	0.520	0.427	0.425
0.083	30.44	3.2E-03	6.5E-03	48	0.510	0.455	0.453
0.250	91.31	9.1E-03	0.018	55	0.439	0.501	0.499
0.500	182.62	0.017	0.034	58	0.408	0.537	0.535
1.000	365.24	0.033	0.063	65	0.337	0.580	0.578
2.000	730.49	0.062	0.114	70	0.286	0.630	0.628
5.000	1826.21	0.134	0.238	74	0.245	0.686	0.683
10	3652.43	0.220	0.374	82	0.163	0.729	0.724
15	5478.64	0.280	0.457	85	0.133	0.756	0.748
20	7304.85	0.324	0.511	87	0.112	0.772	0.761
25	9131.06	0.355	0.546	87	0.112	0.782	0.769
30	10957.28	0.379	0.572	87	0.112	0.789	0.775
35	12783.49	0.398	0.592	89	0.092	0.794	0.779
40	14609.70	0.413	0.605	89	0.092	0.798	0.782
45	16435.91	0.424	0.613	89	0.092	0.801	0.783
50	18262.13	0.431	0.617	89	0.092	0.803	0.784
55	20088.34	0.434	0.619	89	0.092	0.804	0.785
60	21914.55	0.436	0.620	89	0.092	0.804	0.785
Full occ.	Full occ.	1.000	1.000	98	0.000	0.889	0.849

Table S5 – Same as Table S2 for Mw≥5.0 declustered targets (Fig. S3 and S4).

Δt (years)	Δt (days)	τ_u	τ_w	h	ν	$a_f(\tau_u)$	$a_f(\tau_w)$
1.6E-08	5.8E-06	8.6E-10	2.0E-09	0	1.000	0.000	0.000
3.2E-08	1.2E-05	1.7E-09	4.1E-09	0	1.000	0.000	0.000
6.3E-08	2.3E-05	3.4E-09	8.1E-09	0	1.000	0.000	0.000
1.6E-07	5.8E-05	8.6E-09	2.0E-08	0	1.000	0.000	0.000
3.2E-07	1.2E-04	1.7E-08	4.1E-08	0	1.000	0.000	0.000
4.8E-07	1.7E-04	2.6E-08	6.1E-08	1	0.977	0.004	0.004
9.5E-07	3.5E-04	5.1E-08	1.2E-07	1	0.977	0.013	0.013
1.9E-06	6.9E-04	1.0E-07	2.4E-07	1	0.977	0.018	0.018
3.8E-06	1.4E-03	2.0E-07	4.9E-07	2	0.955	0.026	0.026
9.5E-06	3.5E-03	5.1E-07	1.2E-06	2	0.955	0.038	0.038
1.9E-05	6.9E-03	1.0E-06	2.4E-06	2	0.955	0.042	0.042
2.9E-05	1.0E-02	1.5E-06	3.6E-06	2	0.955	0.043	0.043
5.7E-05	2.1E-02	3.0E-06	7.1E-06	2	0.955	0.044	0.044
1.1E-04	4.2E-02	6.0E-06	1.4E-05	2	0.955	0.045	0.045
3.4E-04	0.13	1.7E-05	4.0E-05	4	0.909	0.060	0.060
6.8E-04	0.25	3.4E-05	7.7E-05	4	0.909	0.075	0.075
1.4E-03	0.50	6.5E-05	1.5E-04	4	0.909	0.083	0.082
2.7E-03	1.00	1.3E-04	2.8E-04	4	0.909	0.087	0.087
8.2E-03	3.00	3.6E-04	7.8E-04	6	0.864	0.104	0.104
0.019	7.02	8.1E-04	1.7E-03	7	0.841	0.128	0.128
0.042	15.22	1.7E-03	3.5E-03	7	0.841	0.144	0.144
0.083	30.44	3.2E-03	6.5E-03	8	0.818	0.157	0.156
0.250	91.31	9.1E-03	0.018	8	0.818	0.173	0.172
0.500	182.62	0.017	0.034	10	0.773	0.188	0.187
1.000	365.24	0.033	0.063	14	0.682	0.228	0.227
2.000	730.49	0.062	0.114	19	0.568	0.296	0.294
5.000	1826.21	0.134	0.238	22	0.500	0.387	0.383
10	3652.43	0.220	0.374	29	0.341	0.463	0.455
15	5478.64	0.280	0.457	32	0.273	0.512	0.498
20	7304.85	0.324	0.511	34	0.227	0.544	0.525
25	9131.06	0.355	0.546	34	0.227	0.564	0.541
30	10957.28	0.379	0.572	34	0.227	0.578	0.551
35	12783.49	0.398	0.592	36	0.182	0.588	0.559
40	14609.70	0.413	0.605	36	0.182	0.596	0.565
45	16435.91	0.424	0.613	36	0.182	0.602	0.568
50	18262.13	0.431	0.617	36	0.182	0.606	0.570
55	20088.34	0.434	0.619	36	0.182	0.607	0.571
60	21914.55	0.436	0.620	36	0.182	0.608	0.571
Full occ.	Full occ.	1.000	1.000	44	0.000	0.778	0.699

Table S6 – Same as Table S2 for Mw≥6.0 not-declustered targets (Fig. S5 and S6).

Δt (years)	Δt (days)	τ_u	τ_w	h	ν	$a_f(\tau_u)$	$a_f(\tau_w)$
1.6E-08	5.8E-06	8.6E-10	2.0E-09	0	1.000	0.000	0.000
3.2E-08	1.2E-05	1.7E-09	4.1E-09	0	1.000	0.000	0.000
6.3E-08	2.3E-05	3.4E-09	8.1E-09	1	0.900	0.025	0.025
1.6E-07	5.8E-05	8.6E-09	2.0E-08	1	0.900	0.070	0.070
3.2E-07	1.2E-04	1.7E-08	4.1E-08	1	0.900	0.085	0.085
4.8E-07	1.7E-04	2.6E-08	6.1E-08	1	0.900	0.090	0.090
9.5E-07	3.5E-04	5.1E-08	1.2E-07	1	0.900	0.095	0.095
1.9E-06	6.9E-04	1.0E-07	2.4E-07	1	0.900	0.097	0.097
3.8E-06	1.4E-03	2.0E-07	4.9E-07	2	0.800	0.124	0.124
9.5E-06	3.5E-03	5.1E-07	1.2E-06	2	0.800	0.169	0.169
1.9E-05	6.9E-03	1.0E-06	2.4E-06	3	0.700	0.209	0.209
2.9E-05	1.0E-02	1.5E-06	3.6E-06	3	0.700	0.240	0.239
5.7E-05	2.1E-02	3.0E-06	7.1E-06	3	0.700	0.270	0.269
1.1E-04	4.2E-02	6.0E-06	1.4E-05	3	0.700	0.285	0.284
3.4E-04	0.13	1.7E-05	4.0E-05	4	0.600	0.328	0.327
6.8E-04	0.25	3.4E-05	7.7E-05	5	0.500	0.387	0.386
1.4E-03	0.50	6.5E-05	1.5E-04	5	0.500	0.442	0.440
2.7E-03	1.00	1.3E-04	2.8E-04	5	0.500	0.470	0.469
8.2E-03	3.00	3.6E-04	7.8E-04	6	0.400	0.522	0.521
0.019	7.02	8.1E-04	1.7E-03	7	0.300	0.593	0.591
0.042	15.22	1.7E-03	3.5E-03	7	0.300	0.648	0.646
0.083	30.44	3.2E-03	6.5E-03	7	0.300	0.673	0.671
0.250	91.31	9.1E-03	0.018	7	0.300	0.690	0.690
0.500	182.62	0.017	0.034	7	0.300	0.695	0.694
1.000	365.24	0.033	0.063	8	0.200	0.721	0.720
2.000	730.49	0.062	0.114	8	0.200	0.758	0.756
5.000	1826.21	0.134	0.238	8	0.200	0.780	0.778
10	3652.43	0.220	0.374	9	0.100	0.808	0.804
15	5478.64	0.280	0.457	9	0.100	0.827	0.821
20	7304.85	0.324	0.511	10	0.000	0.844	0.834
25	9131.06	0.355	0.546	10	0.000	0.858	0.844
30	10957.28	0.379	0.572	10	0.000	0.867	0.850
35	12783.49	0.398	0.592	10	0.000	0.873	0.855
40	14609.70	0.413	0.605	10	0.000	0.878	0.857
45	16435.91	0.424	0.613	10	0.000	0.881	0.859
50	18262.13	0.431	0.617	10	0.000	0.883	0.860
55	20088.34	0.434	0.619	10	0.000	0.884	0.860
60	21914.55	0.436	0.620	10	0.000	0.884	0.861
Full occ.	Full occ.	1.000	1.000	10	0.000	0.949	0.911

Table S7 – Same as Table S2 for Mw≥6.0 declustered targets (Fig. S7 and S8).

Δt (years)	Δt (days)	τ_u	τ_w	h	ν	$a_f(\tau_u)$	$a_f(\tau_w)$
1.6E-08	5.8E-06	8.6E-10	2.0E-09	0	1.000	0.000	0.000
3.2E-08	1.2E-05	1.7E-09	4.1E-09	0	1.000	0.000	0.000
6.3E-08	2.3E-05	3.4E-09	8.1E-09	0	1.000	0.000	0.000
1.6E-07	5.8E-05	8.6E-09	2.0E-08	0	1.000	0.000	0.000
3.2E-07	1.2E-04	1.7E-08	4.1E-08	0	1.000	0.000	0.000
4.8E-07	1.7E-04	2.6E-08	6.1E-08	0	1.000	0.000	0.000
9.5E-07	3.5E-04	5.1E-08	1.2E-07	0	1.000	0.000	0.000
1.9E-06	6.9E-04	1.0E-07	2.4E-07	0	1.000	0.000	0.000
3.8E-06	1.4E-03	2.0E-07	4.9E-07	1	0.857	0.036	0.036
9.5E-06	3.5E-03	5.1E-07	1.2E-06	1	0.857	0.100	0.100
1.9E-05	6.9E-03	1.0E-06	2.4E-06	2	0.714	0.157	0.157
2.9E-05	1.0E-02	1.5E-06	3.6E-06	2	0.714	0.200	0.200
5.7E-05	2.1E-02	3.0E-06	7.1E-06	2	0.714	0.242	0.242
1.1E-04	4.2E-02	6.0E-06	1.4E-05	2	0.714	0.264	0.264
3.4E-04	0.13	1.7E-05	4.0E-05	3	0.571	0.325	0.325
6.8E-04	0.25	3.4E-05	7.7E-05	3	0.571	0.375	0.374
1.4E-03	0.50	6.5E-05	1.5E-04	3	0.571	0.401	0.400
2.7E-03	1.00	1.3E-04	2.8E-04	3	0.571	0.414	0.414
8.2E-03	3.00	3.6E-04	7.8E-04	3	0.571	0.424	0.423
0.019	7.02	8.1E-04	1.7E-03	4	0.429	0.466	0.465
0.042	15.22	1.7E-03	3.5E-03	4	0.429	0.520	0.519
0.083	30.44	3.2E-03	6.5E-03	4	0.429	0.545	0.543
0.250	91.31	9.1E-03	0.018	4	0.429	0.562	0.561
0.500	182.62	0.017	0.034	4	0.429	0.567	0.566
1.000	365.24	0.033	0.063	5	0.286	0.603	0.601
2.000	730.49	0.062	0.114	5	0.286	0.654	0.652
5.000	1826.21	0.134	0.238	5	0.286	0.686	0.684
10	3652.43	0.220	0.374	6	0.143	0.725	0.720
15	5478.64	0.280	0.457	6	0.143	0.754	0.744
20	7304.85	0.324	0.511	7	0.000	0.777	0.763
25	9131.06	0.355	0.546	7	0.000	0.797	0.777
30	10957.28	0.379	0.572	7	0.000	0.810	0.786
35	12783.49	0.398	0.592	7	0.000	0.819	0.793
40	14609.70	0.413	0.605	7	0.000	0.825	0.796
45	16435.91	0.424	0.613	7	0.000	0.830	0.799
50	18262.13	0.431	0.617	7	0.000	0.833	0.800
55	20088.34	0.434	0.619	7	0.000	0.834	0.801
60	21914.55	0.436	0.620	7	0.000	0.834	0.801
Full occ.	Full occ..	1.000	1.000	7	0.000	0.928	0.873

2

Table S8 - Results of retrospective forecast of first main shocks (declustered targets) with Mw≥5.0 in Italy from 1960 to 2019, using Δt= 3 months (0.25 years).

Year	Month	Day	Lat	Lon	Mw	t_a (days)		Epicentral area
1960	1	11	41.300	13.983	5.0	Missed		Roccamonfina
1962	8	21	41.233	14.933	5.7	0.093	2.22 h	Irpinia
1963	2	2	42.400	12.900	5.3	0.046	1.10 h	Reatino
1963	2	13	40.500	15.583	5.3	Missed		Potentino
1963	8	9	44.367	12.100	5.4	Missed		Romagna
1965	8	19	46.100	13.100	5.2	Missed		Prealpi friulane
1967	4	3	44.800	10.750	5.0	Missed		Reggiano
1967	10	31	37.800	14.367	5.0	Missed		Monti Nebrodi
1967	12	30	45.000	12.100	5.4	Missed		Emilia Romagna orientale
1968	1	14	37.900	13.000	5.2	Missed		Valle del Belice
1969	11	14	40.583	15.567	5.3	Missed		Potentino
1970	8	19	43.133	10.883	5.0	Missed		Colline Metallifere
1972	11	26	42.900	13.267	5.2	Missed		Marche meridionali
1975	6	19	41.650	15.733	5.1	Missed		Gargano
1975	11	16	44.617	9.433	5.0	Missed		Appennino piacentino
1976	5	6	46.250	13.250	6.5	7.8×10^{-4}	67 s	Friuli
1977	9	16	46.300	12.983	5.3	Missed		Friuli
1978	9	24	40.667	16.117	5.1	Missed		Materano
1979	9	19	42.717	12.950	5.8	Missed		Valnerina
1980	6	14	41.767	13.683	5.0	Missed		Marsica
1980	11	23	40.800	15.367	6.8	Missed		Irpinia-Basilicata
1982	8	15	40.943	15.320	5.3	Missed		Irpinia
1983	11	9	44.653	10.342	5.0	Missed		Parmense
1984	4	29	43.204	12.585	5.6	Missed		Umbria settentrionale
1984	5	7	41.666	13.820	5.9	Missed		Monti della Laga
1990	5	5	40.650	15.882	5.8	1.5×10^{-4}	13 s	Potentino
1991	5	26	40.689	15.822	5.1	Missed		Potentino
1995	9	30	41.790	15.971	5.2	Missed		Gargano
1996	10	15	44.799	10.679	5.4	Missed		Pianura emiliana
1997	9	26	43.023	12.891	5.7	22.1		Appennino umbro-marchigiano
1998	9	9	40.060	15.949	5.5	Missed		Appennino lucano
2002	10	31	41.717	14.893	5.7	Missed		Molise
2003	9	14	44.255	11.380	5.2	Missed		Costa croata settentrionale
2004	11	24	45.685	10.521	5.0	Missed		Garda occidentale
2008	12	23	44.544	10.345	5.4	Missed		Parmense
2009	4	6	42.342	13.380	6.3	6.5		Aquilano
2012	1	25	44.871	10.510	5.0	Missed		Pianura emiliana
2012	5	20	44.896	11.264	6.1	Missed		Pianura emiliana
2012	10	25	39.875	16.016	5.3	Missed		Pollino
2013	1	25	44.164	10.446	5.0	Missed		Garfagnana
2013	12	29	41.395	14.434	5.1	Missed		Matese

2016	*8*	*24*	*42.698*	*13.234*	*6.2*	*Missed*	*Monti della Laga*
2018	8	16	41.874	14.865	5.3	1.9	Molise
2018	12	26	37.644	15.116	5.2	81.1	Etna sud-orientale

t_a is the maximum time advance of the foreshock with respect to the mainshock. "*Missed*" indicates

that the target shock was not forecasted. Epicentral area identifiers are taken from the CPTI15 catalog

(Rovida et al., 2016, 2020).

Table S9 – Results of retrospective forecast of not-declustered targets with Mw≥5.0 in Italy from 1960 to 2019, using Δ*t*= 3 months (0.25 years).

Year	Month	Day	Latitude	Longitude	Mw	t_a(days)
1960	*1*	*11*	*41.3000*	*13.9833*	*5.0*	*Missed*
1962	8	21	41.2333	14.9333	5.7	9.26E-02
1962	8	21	41.2333	14.9333	6.2	9.99E-02
1962	8	21	41.1333	15.1167	5.3	1.17E-01
1963	2	2	42.4000	12.9000	5.3	4.59E-02
1963	*2*	*13*	*40.5000*	*15.5833*	*5.3*	*Missed*
1963	*8*	*9*	*44.3667*	*12.1000*	*5.4*	*Missed*
1965	*8*	*19*	*46.1000*	*13.1000*	*5.2*	*Missed*
1967	*4*	*3*	*44.8000*	*10.7500*	*5.0*	*Missed*
1967	*10*	*31*	*37.8000*	*14.3667*	*5.0*	*Missed*
1967	*12*	*30*	*45.0000*	*12.1000*	*5.4*	*Missed*
1968	*1*	*14*	*37.9000*	*13.0000*	*5.2*	*Missed*
1968	1	15	37.8000	13.2000	5.3	4.05E-01
1968	1	15	37.7000	13.1000	5.7	4.25E-01
1968	1	15	37.8000	13.2000	5.5	9.10E-01
1968	1	16	37.7000	13.3000	5.6	2.03E+00
1968	1	25	37.7000	13.1000	5.2	1.07E+01
1968	*6*	*16*	*37.8000*	*14.8000*	*5.2*	*Missed*
1969	*11*	*14*	*40.5833*	*15.5667*	*5.3*	*Missed*
1970	*8*	*19*	*43.1333*	*10.8833*	*5.0*	*Missed*
1972	*11*	*26*	*42.9000*	*13.2667*	*5.2*	*Missed*
1975	*6*	*19*	*41.6500*	*15.7333*	*5.1*	*Missed*
1975	*11*	*16*	*44.6167*	*9.4333*	*5.0*	*Missed*
1976	5	6	46.2500	13.2500	6.5	7.74E-04
1976	5	11	46.2667	13.0167	5.0	5.10E+00
1976	9	11	46.2667	13.1667	5.3	7.71E+01
1976	9	11	46.3000	13.3167	5.6	8.59E+01
1976	9	15	46.2667	13.1500	5.9	8.05E+01
1976	9	15	46.3000	13.1833	6.0	8.08E+01
1976	9	16	46.2800	12.9800	5.5	8.24E+01
1977	*9*	*16*	*46.3000*	*12.9833*	*5.3*	*Missed*
1978	*9*	*24*	*40.6667*	*16.1167*	*5.1*	*Missed*
1979	*9*	*19*	*42.7167*	*12.9500*	*5.8*	*Missed*
1980	*2*	*28*	*42.8000*	*12.9667*	*5.0*	*Missed*
1980	*6*	*14*	*41.7667*	*13.6833*	*5.0*	*Missed*
1980	*11*	*23*	*40.8000*	*15.3667*	*6.8*	*Missed*
1980	11	24	40.8333	15.2833	5.0	2.30E-01
1980	11	24	40.8667	15.3333	5.0	3.41E-01
1980	11	25	40.6333	15.3833	5.4	1.97E+00
1981	1	16	40.8903	15.4398	5.2	5.32E+01
1982	*8*	*15*	*40.9433*	*15.3202*	*5.3*	*Missed*
1983	*11*	*9*	*44.6525*	*10.3423*	*5.0*	*Missed*
1984	*4*	*29*	*43.2040*	*12.5853*	*5.6*	*Missed*
1984	*5*	*7*	*41.6657*	*13.8202*	*5.9*	*Missed*
1984	5	11	41.6502	13.8437	5.5	3.68E+00
1990	5	5	40.6495	15.8818	5.8	1.46E-04

1991	*5*	*26*	*40.6890*	*15.8217*	*5.1*	*Missed*
1995	*9*	*30*	*41.7903*	*15.9712*	*5.2*	*Missed*
1996	*10*	*15*	*44.7988*	*10.6787*	*5.4*	*Missed*
1997	9	26	43.0228	12.8910	5.7	2.21E+01
1997	9	26	43.0147	12.8538	6.0	2.25E+01
1997	10	3	43.0427	12.8245	5.2	2.95E+01
1997	10	6	43.0275	12.8467	5.5	3.31E+01
1997	10	12	42.9062	12.9203	5.2	3.86E+01
1997	10	14	42.8982	12.8987	5.6	4.07E+01
1998	3	21	42.9485	12.9143	5.0	4.27E+01
1998	3	26	43.1458	12.8090	5.3	4.77E+01
1998	4	3	43.1853	12.7568	5.1	5.53E+01
1998	*9*	*9*	*40.0600*	*15.9490*	*5.5*	*Missed*
2002	*10*	*31*	*41.7167*	*14.8932*	*5.7*	*Missed*
2002	*11*	*1*	*41.7415*	*14.8432*	*5.7*	*Missed*
2003	*9*	*14*	*44.2550*	*11.3800*	*5.2*	*Missed*
2004	*11*	*24*	*45.6850*	*10.5210*	*5.0*	*Missed*
2008	*12*	*23*	*44.5440*	*10.3450*	*5.4*	*Missed*
2009	4	6	42.3420	13.3800	6.3	6.50E+00
2009	4	6	42.3600	13.3280	5.1	6.54E+00
2009	4	6	42.4630	13.3850	5.1	7.41E+00
2009	4	7	42.3360	13.3870	5.1	7.83E+00
2009	4	7	42.3030	13.4860	5.5	8.18E+00
2009	4	9	42.4890	13.3510	5.4	9.47E+00
2009	4	9	42.5040	13.3500	5.2	1.03E+01
2009	4	13	42.4980	13.3770	5.0	1.43E+01
2012	*1*	*25*	*44.8710*	*10.5100*	*5.0*	*Missed*
2012	*5*	*20*	*44.8955*	*11.2635*	*6.1*	*Missed*
2012	*5*	*20*	*44.8787*	*11.1202*	*5.0*	*Missed*
2012	*5*	*20*	*44.9052*	*11.1650*	*5.0*	*Missed*
2012	*5*	*20*	*44.8737*	*11.2703*	*5.2*	*Missed*
2012	5	20	44.8597	11.1520	5.0	3.54E-02
2012	5	20	44.8135	11.4407	5.2	4.62E-01
2012	5	29	44.8417	11.0657	5.9	9.18E+00
2012	5	29	44.8652	10.9795	5.5	1.04E-01
2012	5	29	44.8558	10.9410	5.2	1.07E-01
2012	*10*	*25*	*39.8747*	*16.0158*	*5.3*	*Missed*
2013	*1*	*25*	*44.1643*	*10.4458*	*5.0*	*Missed*
2013	*6*	*21*	*44.1308*	*10.1357*	*5.3*	*Missed*
2013	*12*	*29*	*41.3952*	*14.4342*	*5.1*	*Missed*
2016	*8*	*24*	*42.6983*	*13.2335*	*6.2*	*Missed*
2016	8	24	42.7922	13.1507	5.5	2.60E-02
2016	10	26	42.8747	13.1243	5.5	6.35E+01
2016	10	26	42.9048	13.0902	6.1	6.36E+01
2016	10	30	42.8303	13.1092	6.6	6.71E+01
2016	11	1	42.9902	13.1345	5.0	6.91E+01
2017	1	18	42.5450	13.2768	5.3	8.36E+01
2017	1	18	42.5310	13.2838	5.7	4.97E+01
2017	1	18	42.5033	13.2770	5.6	4.97E+01
2017	1	18	42.4733	13.2747	5.2	4.98E+01
2018	8	16	41.8742	14.8648	5.3	1.86E+00

2

| 2018 | 12 | 26 | 37.6440 | 15.1160 | 5.1 | 8.11E+01 |

t_a is the maximum time advance of the foreshock with respect to the mainshock. "*Missed*" indicates

that the target shock was not forecasted.

Table S10 – Same as Table S9 for not-declustered targets with Mw≥5.5.

Year	Month	Day	Latitude	Longitude	Mw	t_a(days)
1962	8	21	41.2333	14.9333	5.7	9.26E-02
1962	8	21	41.2333	14.9333	6.2	9.99E-02
1968	1	15	37.7000	13.1000	5.7	4.25E-01
1968	1	15	37.8000	13.2000	5.5	9.10E-01
1968	1	16	37.7000	13.3000	5.6	2.03E+00
1976	5	6	46.2500	13.2500	6.5	7.74E-04
1976	9	11	46.3000	13.3167	5.6	8.59E+01
1976	9	15	46.2667	13.1500	5.9	8.05E+01
1976	9	15	46.3000	13.1833	6.0	8.08E+01
1976	9	16	46.2800	12.9800	5.5	8.24E+01
1979	*9*	*19*	*42.7167*	*12.9500*	*5.8*	*Missed*
1980	*11*	*23*	*40.8000*	*15.3667*	*6.8*	*Missed*
1984	*4*	*29*	*43.2040*	*12.5853*	*5.6*	*Missed*
1984	*5*	*7*	*41.6657*	*13.8202*	*5.9*	*Missed*
1984	5	11	41.6502	13.8437	5.5	3.68E+00
1990	5	5	40.6495	15.8818	5.8	1.46E-04
1997	9	26	43.0228	12.8910	5.7	2.21E+01
1997	9	26	43.0147	12.8538	6.0	2.25E+01
1997	10	6	43.0275	12.8467	5.5	3.31E+01
1997	10	14	42.8982	12.8987	5.6	4.07E+01
1998	*9*	*9*	*40.0600*	*15.9490*	*5.5*	*Missed*
2002	*10*	*31*	*41.7167*	*14.8932*	*5.7*	*Missed*
2002	*11*	*1*	*41.7415*	*14.8432*	*5.7*	*Missed*
2009	4	6	42.3420	13.3800	6.3	6.50E+00
2009	4	7	42.3030	13.4860	5.5	8.18E+00
2012	*5*	*20*	*44.8955*	*11.2635*	*6.1*	*Missed*
2012	5	29	44.8417	11.0657	5.9	9.18E+00
2012	5	29	44.8652	10.9795	5.5	1.04E-01
2016	*8*	*24*	*42.6983*	*13.2335*	*6.2*	*Missed*
2016	8	24	42.7922	13.1507	5.5	2.60E-02
2016	10	26	42.8747	13.1243	5.5	6.35E+01
2016	10	26	42.9048	13.0902	6.1	6.36E+01
2016	10	30	42.8303	13.1092	6.6	6.71E+01
2017	1	18	42.5310	13.2838	5.7	4.97E+01
2017	1	18	42.5033	13.2770	5.6	4.97E+01

Table S11 – Same as Table S9 for not-declustered targets with Mw≥6.0.

Year	Month	Day	Latitude	Longitude	Mw	t_a (days)
1962	8	21	41.2333	14.9333	6.2	9.99E-02
1976	5	6	46.2500	13.2500	6.5	7.74E-04
1976	9	15	46.3000	13.1833	6.0	8.08E+01
1980	*11*	*23*	*40.8000*	*15.3667*	*6.8*	*Missed*
1997	9	26	43.0147	12.8538	6.0	2.25E+01
2009	4	6	42.3420	13.3800	6.3	6.50E+00
2012	*5*	*20*	*44.8955*	*11.2635*	*6.1*	*Missed*
2016	*8*	*24*	*42.6983*	*13.2335*	*6.2*	*Missed*
2016	10	26	42.9048	13.0902	6.1	6.36E+01
2016	10	30	42.8303	13.1092	6.6	6.71E+01